Department of Precision and Microsystems Engineering

# Smart Material Actuated Inkjet Printed Robotic Fish

Keerthi Galagali

Report no : 2020. 054
Coach : Dr. A. Hunt, Dr. S. H. HosseinNia
Professor : Prof.dr.ir. J.L. Herder
Specialisation : Mechatronic System Design
Type of report : MSc. Thesis
Date : 27 November 2020

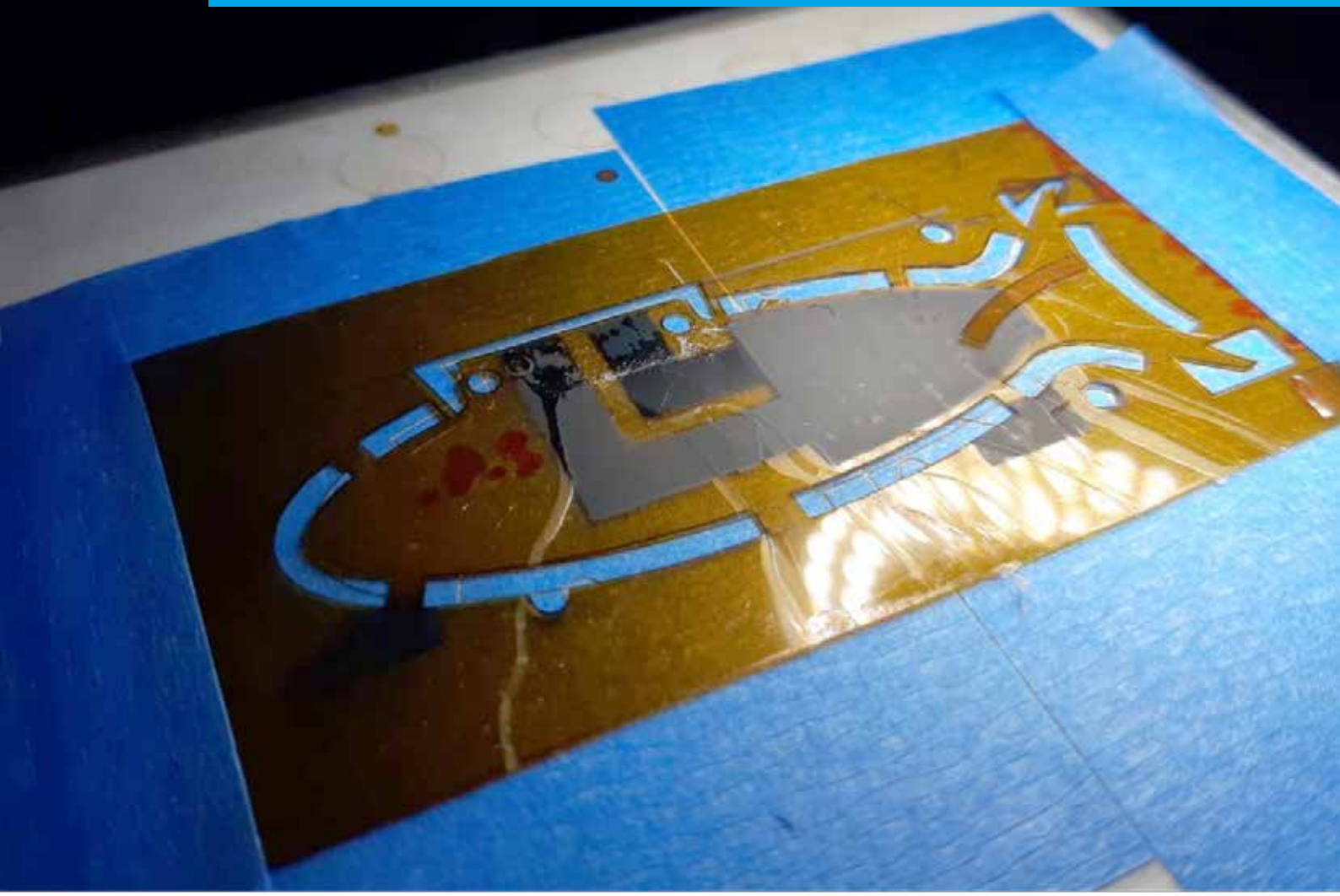

TU Delft Delft University of Technology

Challenge the future

# Smart Material Actuated Inkjet Printed Robotic Fish

by

K. Galagali

to obtain the degree of Master of Science
at the Delft University of Technology,
to be defended publicly on Friday November 27, 2020 at 9:00 AM.

| | | |
|---|---|---|
| Student number: | 4807065 | |
| Project duration: | Sept 2, 2019 – November 27, 2020 | |
| Thesis committee: | Dr. A. Hunt, | TU Delft, Daily Supervisor |
| | Dr. S. H. HosseinNia, | TU Delft, Supervisor |
| | Dr. S. Ghodrat, | TU Delft |

*This thesis is confidential and cannot be made public until November 27, 2022.*



TU Delft

# Contents

# Abstract

Several underwater activities like exploration, surveillance, measuring key characteristics like water current or temperature, and mapping seabed risk human lives as the underwater conditions are hostile. Developing underwater vehicles provides a solution to minimize risking human lives. The underwater robots developed based on conventional actuation tend to be bulky and inefficient, lacking the ability to swim through a complex environment. Using smart materials, efficient robots can be built to swim individually or in swarms through a complex environment. However, there is a huge gap in the performance of the underwater robots developed using smart materials in comparison with the ones actuated conventionally. This thesis fills the gap by elaborating on the development of a robotic fish using polyvinylidene fluoride (PVDF), a smart material, that is proven to produce higher strain per volt among other electro-active polymers (EAPs). To develop a robotic fish, different swimming styles are studied and the carangiform style is adapted to achieve good efficiency without compromising maneuverability. The robotic fish is designed as a monolithic structure with an integrated actuator. The carangiform swimming style is implemented by designing a bi-morph actuator that occupies one-third portion of the robotic fish. The actuator is designed to produce symmetric tail deflections in the lateral direction generating the vortices in the wake which can propel the robotic fish. In order to prove the usability of the actuator underwater, uni-morph actuators were manufactured using the inkjet printing technique. The actuator samples are developed on four different substrate materials, namely PEN, 25$\mu m$ Kapton, 50$\mu m$ Kapton and Novele each with dimensions of 60$mm$x20.5$mm$. Experiments are conducted under various conditions to test their behavior before operating them underwater. The PVDF actuators developed using the Novele substrate successfully operated underwater at an operating frequency of 5.1$Hz$.

# Introduction

Underwater environment can pose several threats to human lives while performing off-shore activities [8]. Underwater robots have the potential to swim through these dangerous environments, collect information and act according to instructions. In the process of developing underwater vehicles, several attempts have been made in the past to imitate existing swimming life forms [11]. While a number of underwater robots have been developed and tested prior, some were developed to prove the application of the technology, and others were developed to improve the performance of the existing underwater robots. The advantage of using bio-mimicry adds value to the design due to optimisation done naturally over the years in nature allowing it to adapt to the existing environmental conditions. The main motivation behind this research is to study the potential of using bio-inspired robots as a tool to help reduce the need for human interaction in dangerous zones underwater.

The first paper of this document records the literature study done to understand the current state of the art of the underwater robots. It is found that there has been a gradual shift from developing conventional motor-driven robotic fishes to smart material actuated robotic fishes in order to reduce the bulkiness and turn the robots into a more efficient and agile system [12]. However, smart material based robots still have a long way to go in proving their performance [10]. The swimming styles adapted by other underwater robots were studied to implement smart material based actuation. The modelling techniques used for developing the robotic fishes so far were reviewed. It is observed that one of the electroactive polymer (EAP), polyvinylidene fluoride (PVDF) was not used by the previously developed robotic fishes. This material showed promising results by producing better strains per volt in comparison to other EAPs [5]. In order to adapt PVDF-based actuation, inkjet printing technique is found to be a suitable manufacturing method. To achieve a balance between thrust and maneuverability, the carangiform swimming style is adopted [15]. It is observed that to develop a printed robotic fish based on PVDF actuation, the state-of-the-art is close to being able to realise it.

Thus, this research aims to develop a miniaturized monolithic robotic fish that can mimic the carangiform swimming style to generate thrust and swim efficiently. This paper fills the gap by designing and developing a PVDF based smart material actuated inkjet printed robotic fish.

The second paper of the document further lays down the path I chose to develop an inkjet printed PVDF actuated robotic fish. The modelling techniques proposed in the paper [6] is proposed to be used for modelling this robot. The challenges faced in the modelling led to a practical design of the robotic fish. A bi-morph actuator is designed to generate symmetric oscillations in the tail part of the robotic fish. On actuation, the oscillating tail is expected to generate vortices in the water that aid in propelling the robotic fish. The size of the robot is based on practical limitations and the shape is based on other carangiform swimmers. In order to test the feasibility of the usage of PVDF actuator underwater, uni-morph actuators are printed to reduce the complexities involved in manufacturing. The actuator samples manufactured are developed using four different substrate materials, namely PEN, 25$\mu m$ Kapton, 50$\mu m$ Kapton, and Novele. The performance of these actuators is tested under different conditions to find its operating frequency, namely without water-

proof coating in the air, with coating in the air, and finally in the water. The operating frequency identified is then used to test the performance of the robotic fish sample.

# II

# A Review on Underwater Robots, Modelling Locomotion and Smart Materials

The paper exhibits the motivation for developing an underwater robotic fish. This literature study describes the current state-of-art of various underwater robotic fishes developed, the trend in the recent past to use smart materials, underwater locomotion including swimming styles and swimming gaits, types of smart materials that could possibly be used, and modelling methods for a robotic fish. The performance of different underwater robots is studied to evaluate the most suitable swimming style. A comparison between the smart materials and their performance is assessed to find a potential material that could be used to develop a robotic fish with improved efficiency. Different modelling techniques are compared to check an adaptable method in order to optimize the performance. Research gaps are identified in this paper to decide the path to be taken to develop a robotic fish.

# Towards Smart Actuated Printed Robotic Fish: Review on underwater robots, modelling fish dynamics and smart actuators

Keerthi Galagali

***Abstract*—Unsafe underwater environment has led to the development of several underwater robots for the past three decades. The underwater robots developed initially tried mimicking different swimming styles of fishes using motors but they were complex in their build with low efficiency. To overcome these shortcomings, smart material actuators have been used in the recent past. While looking at the state of art for underwater robots developed so far, it is observed that the most common electronic EAP - Polyvinylidene fluoride (PVDF) has not been used as an underwater actuator previously. The use of PVDF smart actuator in underwater robots is investigated in this paper due to advantages such as higher bandwidth for same input power with comparable strain performance and its ease of manufacturing using inkjet printing techniques. Printed robots help in reducing intricacies involved in manufacturing while reducing the cost. In order to check the viability of using inkjet printed PVDF actuator as a propelling method for the robotic fish, relevant aspects such as existing underwater robots, suitable swimming styles, modelling and optimizing fish dynamics are looked into. Testing the robotic fish developed would verify if it could achieve the desired efficiency while cruising without compromising the maneuverability.**

***Index Terms*—Underwater robots, Robotic fish, Swimming styles, Modelling and optimizing fish dynamics, Smart actuators, Printed robots, PVDF**

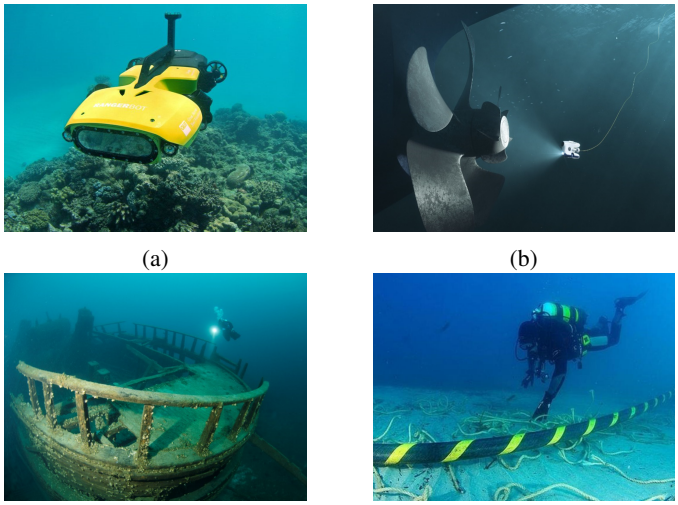

(a) (b) (c) (d)

Fig. 1: Applications of underwater robots: (a) Underwater exploration [7], (b) Port-vessel inspection [5], (c) Ship wreck inspection [8] and (d) Fault detection [9]

## I. INTRODUCTION

The hostile underwater conditions for humans could be avoided by use of underwater robots. Several divers loose their lives while performing underwater activities like ship wreck inspection or while correcting faults in equipment used underwater for off-shore activities [1], [2]. Underwater robots could be used in such hostile conditions for several applications such as exploration/ sea-bed mapping or canal mapping [3], [4], port vessel inspection [5], fault detection in cables or pipelines [4] as depicted in Figure 1 and for swarm robotics in future [6]. To be able to develop an underwater robot for such applications, several aspects such as current state of the art, different actuators used to propel robots in the past, swimming styles that could be adapted, locomotion of a fish and modelling techniques to achieve efficiency and maneuverability of the robotic fish are relevant.

For the past three decades, a number of underwater robots have been developed and tested. While some were developed to prove application of technology, others were developed to improve performance of the existing underwater robots. This paper reviews the underwater robots developed in the past and actuators used by them. It further addresses the gap of using one of the potential smart material actuators [P(VDF-TrFE-CTFE)] to develop a robotic fish to make it commercially viable with ease of manufacturing. Using this smart material is advantageous in terms of manufacturability as it can printed in optimized size of the robot to achieve best possible efficiency. This way, developing this robotic fish could be beneficial by proving an application of technology with a social impact aiming to reduce fatalities underwater.

Starting with the state of art of underwater robots developed so far, the advantages of using smart actuators over conventional motors to propel the underwater robot is highlighted in chapter II. Smart actuated robots are the ones that use smart materials and their properties for actuation. Various swimming styles of natural fishes and how this could be mimicked by robotic fishes is dealt in chapter III. A wide range of available smart materials and the most feasible ones that have been used to develop a robotic fish is presented in chapter IV. It checks the possibility to build a robotic fish using commercial inkjet printer using existing smart materials. For this, the current state of printed robots, materials and manufacturing techniques used for printing smart actuators and sensors is studied. The last chapter deals with the methodology adapted to realise this in

reality by presenting modelling and optimization methods that could be used to build the robotic fish to be tested. A summary of this paper is presented towards the end to highlight the essential details of how a robotic fish can be realized.

## II. UNDERWATER ROBOTS

With numerous applications underwater such as exploration [3], environment sensing [10], research and other commercial purposes, there have been several unmanned underwater vehicles built in the past. They are mainly categorized into Autonomous Underwater Vehicle (AUV) and Remotely Operated Underwater Vehicle (ROV). These underwater robots are required to have characteristics of flexibility or maneuverability, efficiency in speed, good response and safety [11].

The world's first robotic fish developed was Robotuna in 1994, which used DC servo motor to actuate the robot [12]. Other underwater robots like Robotic Eel [13], Nanyang Knifefish [14] and Robotic Knifefish [15] were also driven by several servo motors. The most common actuators robots used were servo motors and hydraulic/pnueumatic actuators in the early stages. Underwater robots like Vorticity Control Unmanned Undersea Vehicle (VCUUV) was driven by hydraulic cylinder while Manta Robot was driven by pneumatic rubber actuator as shown in Figure 2 [12]. The most recent robotic fish developed using servo motor with a compliant/ active body is Robofish L-tail with a max speed of 2.05 BL/s while SoFi was developed by MIT using hydraulic soft robotic system with a speed of 0.51 BL/s [52], [3].

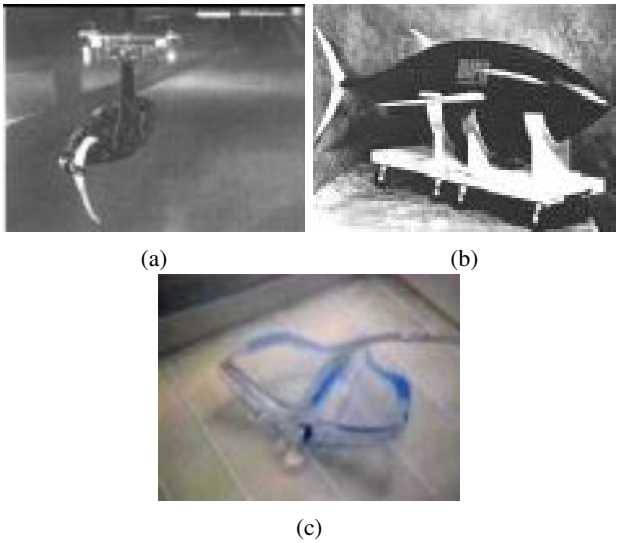

(a) (b)

(c)

Fig. 2: Underwater robots using different actuators (a) DC servo motor actuated Robotuna (b) hydraulic cylinder actuated VCUUV (c) pneumatic actuated Manta Robot [12]

It is evident that underwater robots of numerous forms such as snake-like, jellyfish, eel-like and walking underwater robot have been developed mainly using either electric motors and pneumatic/hydraulic actuators by early 2000s. However, these underwater robots are complex systems with multiple actuators, gearboxes, belts and other mechanical devices to transmit motion to end effectors making them bulky, noisy and less efficient in terms of power consumption [12], [16], [17]. To overcome these shortcomings, researchers adopted an alternative actuation technology by using 'smart' materials to simplify intricacies, reduce weight and dimensions and improve efficiency of the underwater robots. Smart materials such as piezo-electric materials, electro-active polymers [EAPs] and shape memory alloys [SMAs] were observed to have the potential to drive the small sized underwater robots with greater efficiency. Smart actuators have greater ability to perform complex movements with greater flexibility with better response and less noise when compared to conventional actuators [18], [16]. However, the disadvantages of smart actuators is that they are not powerful as servo motors and hence the speed achieved by them will be lesser than robots using conventional actuation [12].

Since 2005, there have been several robotic fishes developed using smart actuators namely IPMC, SMAs and piezo transducers. Table I taken from [18] summarizes different robots built using smart actuators. It can be observed that all types of underwater robots that were mimicked using conventional actuators were developed using smart actuators as well. Robotic fish inspired from tuna actuated by IPMC or PZT, jellyfish-like robot using SMA and ICPF actuators, eel robot using SMA, turtle robot using SSC structure are examples of a wide range of underwater creatures that have been mimicked [18].

| Institute | Actuator | Year |
|---|---|---|
| AIST, Tokyo Institute of technology | IPMC | 2006 |
| Chonnam National University | IPMC | 2009 |
| College of Engineering, Michigan State University | IPMC | 2006 |
| Dankook University and Korea university | IPMC | 2003 |
| Harbin Engineering University and Kagawa University | IPMC | 2008 |
| Harbin Institute of Technology | SMA | 2008, 2009 |
| Kagawa university | SMA, IPMC, Hybrid | 2010, 2003, 2007 |
| Konkuk University | PZT | 2007 |
| Michigan State University | IPMC | 2010 |
| Nagoya University and Kobe University | IPMC | 2006 |
| Northern University | SMA | 2002 |
| Polytechnic Institute of New York University | IPMC | 2010 |
| Seoul National University | SMA | 2011 |
| University of Virginia | IPMC | 2011 |
| Virginia Institute of Technology | SMA | 2011 |

TABLE I: A summary of underwater robots developed using smart actuators (reproduced) [18]

## III. UNDERWATER LOCOMOTION

Underwater creatures have a variety of locomotion methods that could be mimicked. Since ages, fishes have evolved with efficient swimming styles that can be used by underwater robotic fish. The different swimming styles of fishes is presented in this section. An understanding of these swimming methods is important to analyse which style can be best mimicked by striking a balance between maneuverability and thrust generated for propulsion of the robotic fish.

### *A. Swimming styles*

The swimming styles of fishes can be broadly classified into two categories- Body Caudal Fin (BCF) and Median and/or Paired Fin (MPF). This categorization is done based on the parts of the body used for propulsion, that is, BCF swimmers bend their body extending their caudal fins helping them move in propulsive wave while MPF swimmers use their median or pectoral fins to propel. A representation of fins used by fishes for propulsion is depicted in Figure 3.

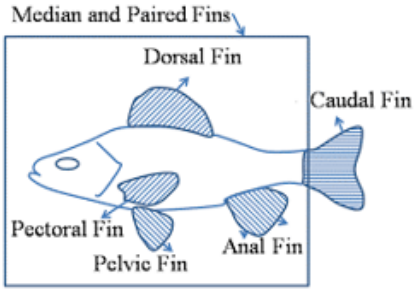


Fig. 3: Representation of fins used by fishes while swimming

Both BCF and MPF swimming styles have a range of movement characteristics varying from undulatory motion to that of oscillatory motion as depicted in Figure 4 [12]. In undulatory motion, the progressive wave passes along the body's propulsive structure allowing maneuverability. While in oscillatory motion, there's a part of progressive wave that swings back and forth to generate thrust in order to propel [19]. Thus, it becomes essential to have a combination of undulatory and oscillatory motion to strike a balance between maneuverability and thrust produced to propel.

*1) Median and/or Paired Fin (MPF):* A very small section of fish families belong to MPF swimmers category. All the swimming forms of MPF swimming forms are considered to provide better stability and maneuverability at slow swimming speeds when compared to BCF swimmers. MPF style of swimming is adopted for achieving movement through structurally complex habitats where speed isn't an important aspect but reaching the target site through maneuverability is essential, like that of coral reef structures [20]. However, MPF swimming style isn't suitable for cruising straight due to its inability to generate speed and thus MPF style is not discussed further.

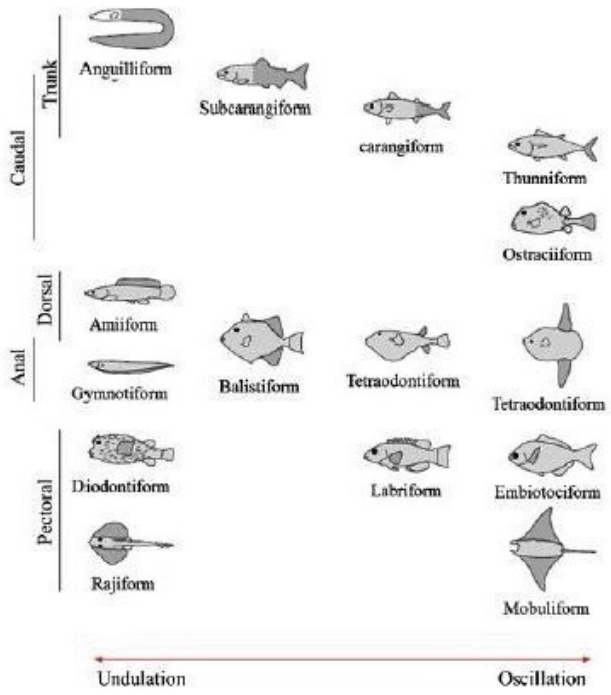


Fig. 4: Categorizing swimming styles [18]

*2) Body Caudal Fin (BCF):* About 85% fish families use BCF swimming style in nature. This makes it convenient to study different forms of swimming in BCF style as illustrated in Figure 5. The swimming styles vary from Anguilliform (eel-like) that swims mostly by undulatory motion to Thunniform which uses oscillatory motion of caudal fins to generate thrust. The style in between Angulliform and Thunniform is the Carangiform which is a combination of undulatory and oscillatory motion. There's one other style called subcarangiform that uses more undulatory motion when compared to oscillatory motion of caudal fin [12].

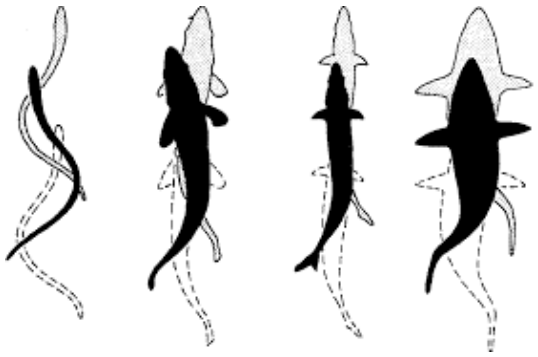

Fig. 5: Variations from undulatory to oscillatory motion in BCF swimming form. Left to right: Auguilliform, Subcarangiform, Carangiform, Thunniform [12]

As it is essential to strike the right balance between maneuverability and thrust for propulsion, carangiform swimming style is the best choice that could be adapted to build a robotic

fish. To adapt the carangiform swimming style, it is required to have about two-third of body flexibility [21], [11]. In the past, the early robotic fish RoboTuna also was built to mimic carangiform [15].

### B. Swimming gait

As discussed in previous section undulatory motion helps in maneuverability while thrust is produced by oscillatory motion of the fins. Most fishes generate a transverse wave that travels down their body to produce thrust. However, the total thrust generated is a combination of two movements, one due to oscillation of tail and the other due to body variations depending on fish's morphology and movements [22], [23] as depicted in Figure 6.

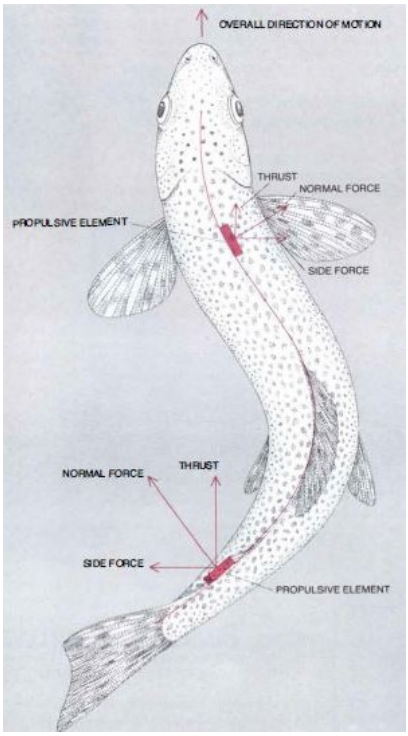


Fig. 6: With the propulsive wave passing down the body, forces act on segments by moving each element laterally and accelerating the water nearby. The normal force exerted on the water has two components: side force and thrust in the direction of overall motion. The magnitude of thrust contributed by each body element increases towards the tail. [23]

Both undulatory and oscillatory swimmers shed vortices in the wake which help in propelling the fish in forward direction. In case of undulatory swimmers, the body undulations create the vortices in the wake resulting in thrust generation while in oscillatory swimmers, the oscillation of caudal fins produce a reverse Karman vortex street resulting in surge of the thrust required to propel [15]. The oscillating motion creates inward vortices on either side producing a peak thrust in the middle behind the fish [52] as depicted in Figure 7.

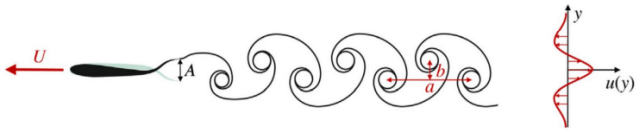


Fig. 7: Illustration of reverse Karman vortex street generation [52]

### C. Swimming modes

The most common swimming modes experimented after understanding the swimming gait of a fish are:

- Cruise-straight or steady swimming
- Cruise turn-in
- Ascent or descent

The acceleration and deceleration are other complex swimming modes tested to check the performance of the robotic fish [16], [24], [25], [4], [26].

In case of cruise-straight, the amplitude of oscillation of the caudal fin is the constant laterally on either side of the body while it varies in amplitude for cruise turn-in mode [16], [27]. The complications of locomotion increase from straight-cruise to that of cruise turn-in or ascent and descent. The primary goal is to achieve the steady swim or cruise-straight before introducing further complexities in the robotic fish to be developed.

## IV. SMART ACTUATORS

This section gives basic information on smart materials available. The most used smart materials for underwater robotics is discussed with their pros and cons. The smart material that can produce large amplitude strains to generate vortices in the wake which can propel the robotic fish would be used to develop the underwater robot. Further, the smart material that can be used for building the robotic fish by inkjet printing is proposed along with the challenges involved.

### A. Smart materials

Smart materials are those that connect a state variable in one domain to a state variable from a different physical domain. The physical domains are mechanical, electrical, thermal, magnetic, optical and chemical. Any physical domain can be described by two state variables, like stress and strain could be used to define mechanical domain [28]. While considering only mechanical physical domain to generate output to produce required deflection to propel the micro-robot, the smart materials studied are of the following categories: electro-mechanical, thermo-mechanical, magneto-mechanical, photo-mechanical and chemical mechanical [6]. Other source of actuation such as biological actuation are not considered [28]. A mindmap of all smart materials is well in [29] where all the domains and their sub categories are put together as represented in Figure 8.

There have been instances where shape memory alloys (SMAs) from thermo-mechanical domain have been used for underwater robotics as mentioned in Table I, adapted from the

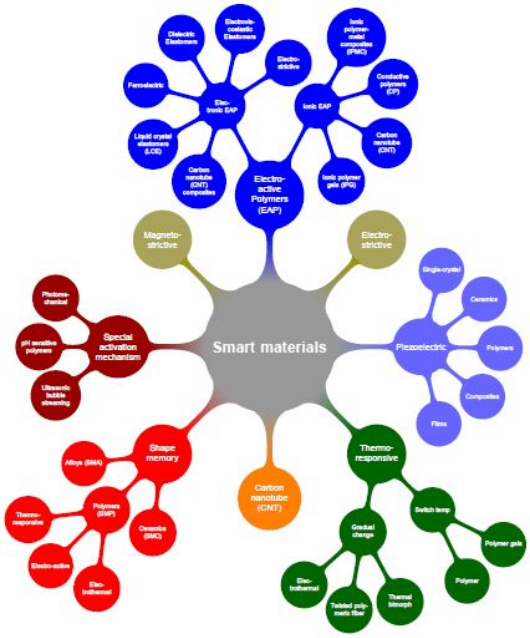


Fig. 8: A mindmap of Smart materials [29]

review paper on Biomimetic Underwater Robots using smart materials [18]. However, the smart materials from electro-mechanical domain is possibly more interesting due to their ability to induce large strains when compared to other physical domains. The piezoelectric materials and other electro-active polymers (EAPs) are some examples of this domain. Though piezoelectric materials are a large group in smart actuators, they produce small strains for relatively large forces [29]. Thus, is not well suited for swimming applications. Therefore, we look into EAPs as they produce better strains when compared to piezoelectric materials. An overview of EAPs being used for robotic applications as sensors and actuators have been presented in [30].

EAPs can be further categorized in two ways: electronic EAP and ionic EAP. There have been several instances in the past where ionic EAP, IPMC in particular, has been used for underwater robot applications. A lot of IPMC related underwater robotic applications can be found listed in [31] by A. Hunt. The design and optimization of IMPC actuated swimming tail has been explored as well [29]. A combination of SMA and IMPC have also been used in some cases and these swimming actuators are called as hybrid due to the combination of different smart actuators [18]. The difficulties in using multiple materials for actuation are addressed in [32].

However, the application of electronic EAP has not been explored much for underwater robots which could be advantageous in terms of larger displacement range and quick response when compared to IPMC or SMAs. A polymer based robotic fish was developed using Polypyrrole (PPy) but was concluded to have weak actuation with other limitations [33]. Polyvinylidene fluoride (PVDF) is one of the most commonly used ferroelectric polymer. There are certain shortcomings of PVDF, such as, it requires high voltage to produce strains and have heat dissipation issues [28] while there are more advantages as it is easy to manufacture it economically by printing it using commercial inkjet printers [34].

While PVDF is the base polymer, several attempts have been made to improve the properties by adding of monomers to achieve better strains. Inclusion of TrFE monomer in PVDF results in P(VDF-TrFe) which helps in improving electro-mechanical properties allowing better sensitivity when used in transducers [35], [36]. By addition of chlorine atom into the monomer, the electromechanical strains achieved were greater than 5%. Thus, P(VDF-TrFe-CTFE) helped in eliminating dielectric heating and poling hysteresis by achieving higher polarization of monomer pairs [37]. These properties of P(VDF-TrFe-CTFE) makes it suitable for thin flexibe actuators that could be manufactured using inkjet printing [34].

### *B. Manufacturing P(VDF-TrFe-CTFE) by inkjet printing*

Printing technology for manufacturing has been more widely used presently than other conventional techniques. This comes with advantages such as low wastage during manufacturing, easy production techniques, customized prototype production viability and improved performance when compared to products manufactured by conventional methods. There exists printing technology from large scale in form of 3D printing to that of small scale printing using inkjet printers [21].

Since, the goal is to produce the robot in small scale economically, the focus is shifts towards inkjet printing instead of other printing technologies as inkjet printing manufacturing technique allows miniaturization with added advantage of being able to produce economical micro-robots. Both conductive and electroactive materials can be printed using inkjet printers. An inkjet printed paper robot has been reported of the size 35 $mm$ x 15 $mm$ x 10 $mm$ using silver ink in a 2D pattern to induce self-folding [38].

While most ferroelectric polymer actuators used silver conductive layer and P(VDF-TrFE) electroactive material, recently P(VDF-TrFE-CTFE) with carbon black electrodes has been proven to produce improved strains with ease of manufacturing when compared to silver conductive layers. P(VDF-TrFE-CTFE) with carbon electrodes achieve $206\,\mu\mathrm{m}$ deflection at 300V and $3\,\mathrm{mm}$ at resonance [34]. The different layers printed to produce a PVDF actuator are represented in Figure 9.

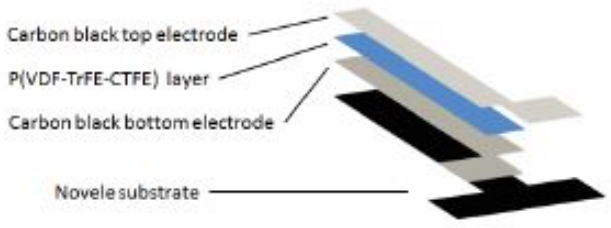


Fig. 9: PVDF actuator in layered structure [34]

The steps involved in manufacturing PVDF actuator is represented in Figure 10 with details of temperature and time required to cure to achieve the end result. The positive side of using P(VDF-TrFe-CTFE) as an actuator is that it does not require any post processing making it a suitable material to develop the robotic fish by inkjet printing [34], [36].

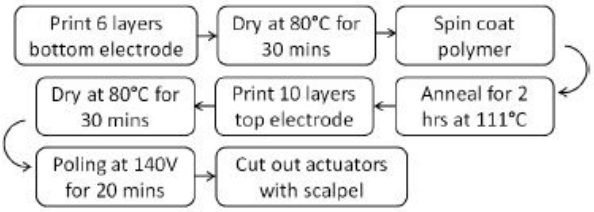


(a)

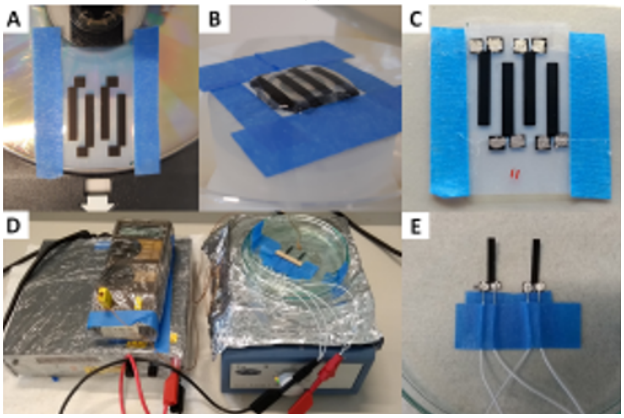


(b)

Fig. 10: (a) Steps involved in manufacturing PVDF actuator (b) Making of P(VDF-TrFe-CTFE) actuator [34]

## V. MODELLING AND PERFORMANCE OPTIMIZATION

With the challenge to build an efficient and maneuverable underwater robotic fish, it is necessary to choose an appropriate modelling technique and optimize it. The development of robotic fishes includes not just kinematic modelling of the robot but is also affected by hydrodynamic environment modelled around it. The combination of both models together help in realizing the complete model that could be used to optimize the efficiency of the robotic fish. This isn't easy due to the problems faced in coupling the robot's structural movement with the surrounding environment [25].

### *A. Modelling robotic fish*

Researchers have made several attempts to formulate models that best describes the kinematics of a fish. The kinematic modelling of the robotic fish is done for the body and its tail, either as a multi-linked body as in [24], [39], [40] or using flexible body and a complaint tail as mentioned in [26], [41] along with other examples mentioned in the same paper. In both cases we have a problem of an optimal design. In case of compliant body design, finding the elasticity values and distribution of the body is critical. In case of multilink robot, deciding the number and the stiffness of the links is critical [42].

In case of multi-linked body, generally, several actuators are used to actuate each link independently as in case of [43], [13] or [24] while in case of compliant body, approximation techniques or discretization are used as it is difficult to model an exact solution for the real system. There are three discretization formulations presented in [41]:

- Assumed modes method
- Finite element method
- Lumped parameter method

A variety of modelling techniques such as analytical, numerical, simulation based such as modal analysis or finite element method (FEM) based model are available. The modelling technique adapted should be able to make use of a simplified model which could be used for real-time computation. This section presents examples of modelling techniques used by researchers in the past while developing a robotic fish.

The multi-linked body modelling technique was adapted in [24] where modelling was done in three parts: joint kinematic model of the fish, hydrodynamic model using added mass method and kinematic modelling combining both joint kinematic model with that of hydrodynamic model. Mathematical models were used to describe the fish tail's transverse displacement using a travelling wave while assumptions like quasi-static fluid and only drag force due to viscosity were considered to simplify the added mass hydrodynamic model.

The multi-linked body models have been applied and further integrated in real time by using an extension of the Newton–Euler recursive forward dynamics algorithm for manipulators to a robot without a fixed base [43]. A schematic of a robotic fish's internal kinematics with multiple joints has been represented in Figure 11. There have also been hybrid algorithms developed to amalgamate the dynamics with that of controls using Newton- Euler approach to compute net motion and body deformations and torques at intermediate joints in case of discretised rigid bodies [44].

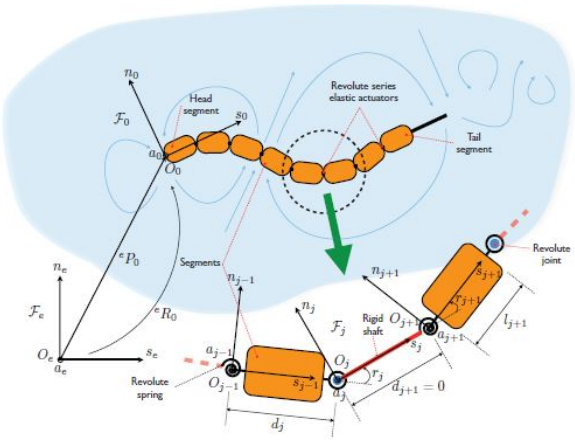


Fig. 11: Schematic representation of internal kinematics of fish-like swimming [43]

El Daou et al. [41] used an energetic approach based on 'assumed modes method' to come up with equations of motion for compliant body. Reyleigh's damping model was used to compute hydrodynamic forces in experiments. This paper used modal analysis technique as depicted in Figure 12 to compute the relationship between applied moments and lateral deflections in the body of the fish. This formulation technique of 'assumed modes' is suitable for systems with simpler cross section geometry and with one flexible link only.

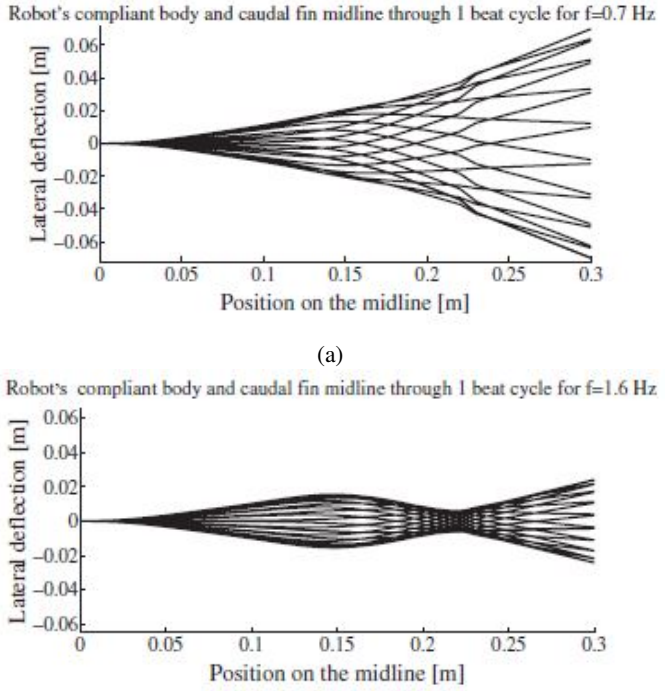


(a)

(b)

Fig. 12: Robot's compliant body and caudal fin midline for different frequencies [41]

Shahinpoor et al. [45] used analytical equations to study continuum microelectromechanical model of IPMC actuator and carried out numerical simulations to find dynamic behaviour of actuator to compare the results with experiment. This method is useful when study of actuator behaviour is done in detail but not when dynamics of robotic fish is more relevant.

Piezo based Bionic Robotic fish developed by Zhang [25] used modal analysis to obtain the modal frequency and vibration of the robotic fish structure. However, the modal analysis did not consider the influence of environment. This was solved by using acoustic-solid coupling algorithm. In this case, FEM method was used to simulate and analyse the coupling between deformation of the structure and how it was affected by the fluid pressure around it while the modal analysis was used to see how the bionic fish responded to different frequency input signals.

Shirgaonkar et al. [46] used a three dimensional (3D) computational fluid dynamics (CFD) simulation to study the hydrodynamics of an undulating ribbon fin. While a mix of analytical and CFD methods have been used for modelling by Anton et al. [42]. A depiction of FEM based analysis using CFD is represented in Figure 13. However, FEM based models are computationally expensive and are not of much use for real-time simulations. They are recommended for flexible multi-linked body with complex cross-sectional geometries [41].

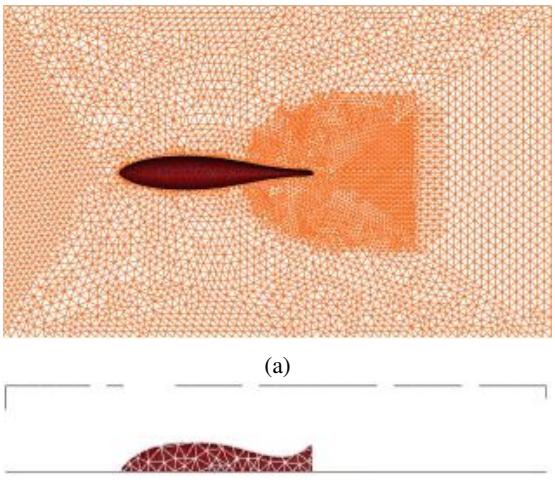

(a)

(b)

Fig. 13: (a) Top view of fluid domain (b) Side view of fluid domain with flow from left to right, robot has a wall boundary while others are slip boundaries [42]

The lumped parameter method uses pseudo joints and linear springs to model the flexibility of compliant parts. This technique is similar to multi-linked body method and is simple when compared to FEM or assumed modes method. However, the difficulty with both multi-linked body method and lumped parameter method is finding the optimum number of joints and spring constants [41].

### *B. Hydrodynamic model*

The hydrodynamic modelling involves fluid properties and its effects on the surface of the robotic fish [47]. To model interaction between the robotic fish and it's surrounding environment, Lighthill's model is usually adapted along with slender body theory [47], [48]. For more realistic approach, Lighthill developed a generalized analytical model to cater arbitrary amplitude of fish's motion based on large amplitude elongated body theory (LAEBT) which is more apt for carangiform swimmers [43].

The hydrodynamic forces are either modelled in terms of added mass or in terms analogous to viscous damping. While mostly added mass method is used to model hydrodynamic forces as in case of [24], [4], there have been instances where damping method has been used as in case of [41].

The main hydrodynamic forces considered are- thrust and drag, in horizontal plane along the direction of motion of the robotic fish. The vertical forces to be balanced are weight

of the robotic fish with the buoyancy forces [47]. However, vertical forces would play a major role in case of accent or decent of the robotic fish but in this paper only straight-cruise is focused upon. The main challenge in hydrodynamic design is to come up with a low drag design during locomotion with appropriate buoyancy to weight distribution [3].

The overall thrust generated is given by forward forces propelling the robotic fish minus the resistive forces acting in the opposite direction. The major drag forces are either reactive drag forces or resistive drag forces [43]. These are due to reactions in water due to movement of fins of the fish or due to viscous and other drag resistance offered around the fish. The viscous drag is given by Equation 1 and is dependent on a coefficient.

$$D = 1/2\ C_f S V^2 \rho \tag{1}$$

where, $C_f$ is drag coefficient that depends on Reynolds number, S is the wet surface area and $\rho$ is density of the fluid (water).

In case of steady state, Reynold's number helps in describing the fluid's characteristics and its effects on the flowing body. However, in unsteady state with oscillations occuring at a frequency generating wakes for the fish, Strouhal number given by the Equation 2 holds importance. This characterizes the ratio of unsteady to inertia forces [47].

$$S_t = f A_{tail}/V \tag{2}$$

where $S_t$ represents Strouhal number, $f$ represents frequency of oscillation and $A_{tail}$ represents amplitude of oscillation and $V$ is the forward velocity. The nominal range lies in the range 0.25 to 0.35 [16], [24], [47]. Strouhal number is physically interpreted as the ratio between flapping velocity of trailing edge to that of flow velocity altered due to flapping [19]. It is notable that drag reduces with increased Strouhal number till 0.3 [48].

Studies have been conducted on vortex shedding and the generation of wake of the fish to visualize the flow in channels and how this helps in propulsion of the fish [49], [22], [50]. These studies have helped in understanding the hydrodynamic effect on the robotic fish in a better way.

The combination of modelling both kinematic and hydrodynamic together in order to couple flexible motion of the robotic fish with hydrodynamic environment requires a simplified model that is inexpensive in terms of computation. However, care has to be taken to not over-simplify the model deviating from realistic scenario.

### C. Optimization

The motive of modelling the robotic fish is being able to ease optimization of its performance to achieve best possible efficiency and speed while cruising straight. In some cases, parameters of the robotic fish were optimized to find the best performance for different swimming modes [4]. However, this paper presents several parameters that can be considered for optimization, the main parameters are structural parameters of the robotic fish and hydrodynamic properties that affect the performance of the fish.

The structural properties of the fish that can be parametric are body length [42], max height [25], caudal fin height [25], total mass [25], [27], cross-section of robotic fish and flexibility ratio. The actuator size is relevant as well as the strains achieved at resonance frequencies varies accordingly [34], [25]. An algorithm to find optimized link lengths and number of links have been provided by [42].

Other parameters such as voltage supply with respect to time [27], natural frequency in water [41], maximum amplitude of oscillation and oscillation frequency affect the performance of the robotic fish [42]. Fluid properties such as density of the fluid [25], Strouhal's number and drag forces acting on the fish are other parameters that influence the efficiency of the robotic fish. While most of these parameters act as constraints, variables like number of links and voltage supply can be varied to optimize the performance of the fish.

## VI. DISCUSSIONS

There have been several purposes due to which many underwater robots have been built in the past. Research and exploration being important underwater applications, there have been instances where several sensors have been used onboard to help capturing required data underwater using varied actuators [10], [51], [21]. Thus, in order to develop a robotic fish, advances made in existing underwater robots, swimming styles, modelling methods and potential manufacturing techniques using smart actuators are reviewed.

While the first robotic fish development was sparked in the year 1994, research intensified significantly in 2000s. Initially built robotic fishes were rigid mechanical systems actuated mostly by motors while the more recent trends go towards more compact mechanical design using smart materials actuators. While the concept has plenty of interest, it seems to be that cost of large robotic fish and manufacturability of the smart actuators are the ones to be holding back wide-spread utilisation.

Regarding swimming styles, literature shows that biologists have thoroughly studied them since 1960s. Robotic fish researchers have implemented both MPF and BCF styles, but the most versatile seems to be carangiform or subcarangiform of BCF style, since it allows to achieve both cruise and maneuverability at relatively low design complexity. The same style - carangiform is most relevant for propelling a printed robotic fish as well in future.

With a wide range of smart materials available, the most used ones by researchers are from electro-mechanical domain or thermo-mechanical domain. Piezo transducers, SMAs and IPMC are the most commonly used smart materials in the past by the robotic fish developers. However, P(VDF-TrFe-CTFE) with high strain producing capacity that can be manufactured by inkjet printing technology is seen as a potential smart actuator to propel the robotic fish.

Regarding performance of the robotic fish, several models are available that could be used for optimization of speed and efficiency. Many researchers have used varied modelling techniques like analytical models [45], numerical simulations

[45], computational models based on FEM [42] or modal analysis [41] to determine performance of the robotic fish. The model developed by Lighthill has been most adapted and used by researchers to study the interaction between robotic fish and surrounding water. Lighthill's model is adapted to compute the performance for futuristic printed robotic fish as well. However, the computational technique would be a simplified modular model in order to be able to adapt it in real-time. This model could be used to optimize results by controlling variables and constraints to achieve best possible speed while cruising straight.

## VII. CONCLUSIONS

It is seen that to develop a printed robotic fish based on smart material actuation, the state-of-the-art is close to being able to realise them. It is possible to adapt carangiform swimming style for propulsion to achieve a balance between thrust and maneuverability using P(VDF-TrFe-CTFE) material. This material is proven to have great strains among other smart actuators and can be manufactured by inkjet printing technology. For performance optimization, there exist several usable modelling techniques. It is essential to adapt to a simplified model that is computationally not demanding to be able to optimize the performance of the robotic fish in real-time. All the above aspects put together will lead towards realising a smart actuated printed underwater robotic fish.

## REFERENCES


[1] P. Buzzacott, *DAN Annual Diving Report 2017 Edition: A Report on 2015 Diving Fatalities, Injuries, and Incidents*. Divers Alert Network, 2017.

[2] P. Buzzacott and D. A. Network, "Dan annual diving report," *Divers Alert Network: Durham, NC, USA*, 2015.

[3] R. K. Katzschmann, J. DelPreto, R. MacCurdy, and D. Rus, "Exploration of underwater life with an acoustically controlled soft robotic fish," *Science Robotics*, vol. 3, no. 16, p. eaar3449, 2018.

[4] H. Hu, "Biologically inspired design of autonomous robotic fish at essex," in *IEEE SMC UK-RI Chapter Conference, on Advances in Cybernetic Systems*, 2006, pp. 3–8.

[5] "Eggs exhibiting at nor-shipping 2019," https://eggsdesign.com/stories/read/eggs-exhibiting-at-nor-shipping-2019, Accessed: 2020-01-29.

[6] L. Hines, K. Petersen, G. Z. Lum, and M. Sitti, "Soft actuators for small-scale robotics," *Advanced materials*, vol. 29, no. 13, p. 1603483, 2017.

[7] "Robot reef protector sees a new way to check great barrier reef health," https://phys.org/news/2018-08-robot-reef-protector-great-barrier.html, Accessed: 2020-01-29.

[8] "Consent form — scuba diving," https://www.scubadiving.com/drive-and-dive-exploring-wrecks-tobermory, Accessed: 2020-01-29.

[9] "Convenzione sorrento-terna per investimenti in opere di pubblica utilità - telestreet arcobaleno," https://telestreetarcobaleno.tv/convenzione-sorrento-terna-per-investimenti-in-opere-di-pubblica-utilita/, Accessed: 2020-01-29.

[10] Y.-S. Ryuh, G.-H. Yang, J. Liu, and H. Hu, "A school of robotic fish for mariculture monitoring in the sea coast," *Journal of Bionic Engineering*, vol. 12, no. 1, pp. 37–46, 2015.

[11] S. Guo, T. Fukuda, N. Kato, and K. Oguro, "Development of underwater microrobot using icpf actuator," in *Proceedings. 1998 IEEE International Conference on Robotics and Automation (Cat. No. 98CH36146)*, vol. 2. IEEE, 1998, pp. 1829–1834.

[12] A. A. M. Faudzi, M. R. M. Razif, N. A. M. Nordin, E. Natarajan, and O. Yaakob, "A review on development of robotic fish," *Journal of Transport System Engineering*, vol. 1, no. 1, pp. 12–22, 2014.

[13] K. Low, G. G. Seet, and C. Zhou, "Biomimetic design and workspace study of compact and modular undulating fin body segments," in *2007 International Conference on Mechatronics and Automation*. IEEE, 2007, pp. 129–134.

[14] K. Low, C. Zhou, G. G. SEET, and J. Yu, "Learning from gymnotiform swimmers—design and implementation of robotic knifefish nkf-ii," *International Journal of Information Acquisition*, vol. 5, no. 02, pp. 137–147, 2008.

[15] I. D. Neveln, Y. Bai, J. B. Snyder, J. R. Solberg, O. M. Curet, K. M. Lynch, and M. A. MacIver, "Biomimetic and bio-inspired robotics in electric fish research," *Journal of experimental Biology*, vol. 216, no. 13, pp. 2501–2514, 2013.

[16] C. Rossi, W. Coral, J. Colorado, and A. Barrientos, "A motor-less and gear-less bio-mimetic robotic fish design," in *2011 IEEE International Conference on Robotics and Automation*. IEEE, 2011, pp. 3646–3651.

[17] C. Rossi, A. Barrientos, and W. C. Cuellar, "Sma control for bio-mimetic fish locomotion." in *ICINCO (2)*, 2010, pp. 147–152.

[18] W.-S. Chu, K.-T. Lee, S.-H. Song, M.-W. Han, J.-Y. Lee, H.-S. Kim, M.-S. Kim, Y.-J. Park, K.-J. Cho, and S.-H. Ahn, "Review of biomimetic underwater robots using smart actuators," *International journal of precision engineering and manufacturing*, vol. 13, no. 7, pp. 1281–1292, 2012.

[19] W. Tey and N. C. Sidik, "Comparison of swimming performance between two dimensional carangiform and anguilliform locomotor," *Journal of Advanced Research in Fluid Mechanics and Thermal Sciences*, vol. 11, pp. 1–10.

[20] K. E. Korsmeyer, J. F. Steffensen, and J. Herskin, "Energetics of median and paired fin swimming, body and caudal fin swimming, and gait transition in parrotfish (scarus schlegeli) and triggerfish (rhinecanthus aculeatus)," *Journal of experimental biology*, vol. 205, no. 9, pp. 1253–1263, 2002.

[21] A. Raj and A. Thakur, "Fish-inspired robots: design, sensing, actuation, and autonomy—a review of research," *Bioinspiration & biomimetics*, vol. 11, no. 3, p. 031001, 2016.

[22] U. K. Müller, J. Smit, E. J. Stamhuis, and J. J. Videler, "How the body contributes to the wake in undulatory fish swimming: flow fields of a swimming eel (anguilla anguilla)," *Journal of Experimental Biology*, vol. 204, no. 16, pp. 2751–2762, 2001.

[23] P. W. Webb, "Form and function in fish swimming," *Scientific American*, vol. 251, no. 1, pp. 72–83, 1984.

[24] J. Liu and H. Hu, "A 3d simulator for autonomous robotic fish," *International Journal of automation and computing*, vol. 1, no. 1, pp. 42–50, 2004.

[25] C. Zhang, "Simulation analysis of bionic robot fish based on mfc materials," *Mathematical Problems in Engineering*, vol. 2019, 2019.

[26] Y. Zhong, Z. Li, and R. Du, "A novel robot fish with wire-driven active body and compliant tail," *IEEE/ASME Transactions on Mechatronics*, vol. 22, no. 4, pp. 1633–1643, 2017.

[27] D. Chen, W. Shao, and C. Xu, "Development of a soft robotic fish with bcf propulsion using mfc smart materials," in *2018 37th Chinese Control Conference (CCC)*. IEEE, 2018, pp. 5358–5363.

[28] M. Freriks, "Design and modelling of IPMC kirigami: for distributed actuation," 2019.

[29] L. Boerefijn, "IPMC actuator for swimming microrobots," 2017.

[30] K. J. Kim and S. Tadokoro, "Electroactive polymers for robotic applications," *Artificial Muscles and Sensors*, vol. 23, p. 291, 2007.

[31] A. Hunt, "Application-oriented performance characterization of the ionic polymer transducers (ipts)," Ph.D. dissertation, Ph. D. Thesis, Tallinn University of Technology, Tallinn, Estonia, 2017.

[32] M. R. Cutkosky and S. Kim, "Design and fabrication of multi-material structures for bioinspired robots," *Philosophical Transactions of the Royal Society A: Mathematical, Physical and Engineering Sciences*, vol. 367, no. 1894, pp. 1799–1813, 2009.

[33] H. Wang, S. S. Tjahyono, B. MacDonald, P. A. Kilmartin, J. Travas-Sejdic, and R. Kiefer, "Robotic fish based on a polymer actuator," in *Proc. Australasian Conf. on Robotics and Automation (Brisbane, December)*, 2007, pp. 1809–13.

[34] K. Baelz, "P(VDF-TrFe-CTFE) actuators with inkjet printed electrodes," 2019.

[35] H. Ohigashi, K. Koga, M. Suzuki, T. Nakanishi, K. Kimura, and N. Hashimoto, "Piezoelectric and ferroelectric properties of P (VDF-TrFE) copolymers and their application to ultrasonic transducers," *Ferroelectrics*, vol. 60, no. 1, pp. 263–276, 1984.

[36] R. van der Nolle, "Production, design and control of p (vdf-trfe-ctfe) relaxor-ferroelectric actuators," 2017.
[37] H. Xu, Z.-Y. Cheng, D. Olson, T. Mai, Q. Zhang, and G. Kavarnos, "Ferroelectric and electromechanical properties of poly (vinylidene-fluoride–trifluoroethylene–chlorotrifluoroethylene) terpolymer," *Applied Physics Letters*, vol. 78, no. 16, pp. 2360–2362, 2001.
[38] H. Shigemune, S. Maeda, V. Cacucciolo, Y. Iwata, E. Iwase, S. Hashimoto, and S. Sugano, "Printed paper robot driven by electrostatic actuator," *IEEE Robotics and Automation Letters*, vol. 2, no. 2, pp. 1001–1007, 2017.
[39] K. A. McIsaac and J. P. Ostrowski, "Motion planning for anguilliform locomotion," *IEEE Transactions on Robotics and Automation*, vol. 19, no. 4, pp. 637–652, 2003.
[40] S. D. Kelly, R. J. Mason, C. T. Anhalt, R. M. Murray, and J. W. Burdick, "Modelling and experimental investigation of carangiform locomotion for control," in *Proceedings of the 1998 American Control Conference. ACC (IEEE Cat. No. 98CH36207)*, vol. 2. IEEE, 1998, pp. 1271–1276.
[41] H. El Daou, T. Salumäe, L. D. Chambers, W. M. Megill, and M. Kruusmaa, "Modelling of a biologically inspired robotic fish driven by compliant parts," *Bioinspiration & biomimetics*, vol. 9, no. 1, p. 016010, 2014.
[42] M. Anton and M. Listak, "Hydrodynamic optimization of a relative link lengths for a biomimetic robotic fish," in *2011 15th International Conference on Advanced Robotics (ICAR)*. IEEE, 2011, pp. 530–535.
[43] M. Porez, F. Boyer, and A. J. Ijspeert, "Improved lighthill fish swimming model for bio-inspired robots: Modeling, computational aspects and experimental comparisons," *The International Journal of Robotics Research*, vol. 33, no. 10, pp. 1322–1341, 2014.
[44] M. Porez, F. Boyer, and A. Belkhiri, "A hybrid dynamic model for bio-inspired soft robots—application to a flapping-wing micro air vehicle," in *2014 IEEE International Conference on Robotics and Automation (ICRA)*. IEEE, 2014, pp. 3556–3563.
[45] M. Shahinpoor and K. J. Kim, "Ionic polymer–metal composites: Iii. modeling and simulation as biomimetic sensors, actuators, transducers, and artificial muscles," *Smart materials and structures*, vol. 13, no. 6, p. 1362, 2004.
[46] A. A. Shirgaonkar, O. M. Curet, N. A. Patankar, and M. A. MacIver, "The hydrodynamics of ribbon-fin propulsion during impulsive motion," *Journal of Experimental Biology*, vol. 211, no. 21, pp. 3490–3503, 2008.
[47] M. Sfakiotakis, D. M. Lane, and J. B. C. Davies, "Review of fish swimming modes for aquatic locomotion," *IEEE Journal of oceanic engineering*, vol. 24, no. 2, pp. 237–252, 1999.
[48] M. S. Triantafyllou, G. Triantafyllou, and D. Yue, "Hydrodynamics of fishlike swimming," *Annual review of fluid mechanics*, vol. 32, no. 1, pp. 33–53, 2000.
[49] H. Sakamoto and H. Haniu, "A study on vortex shedding from spheres in a uniform flow," 1990.
[50] I. J. Sobey, "Oscillatory flows at intermediate strouhal number in asymmetric channels," *Journal of Fluid Mechanics*, vol. 125, pp. 359–373, 1982.
[51] J. Yu, S. Chen, Z. Wu, and W. Wang, "On a miniature free-swimming robotic fish with multiple sensors," *International Journal of Advanced Robotic Systems*, vol. 13, no. 2, p. 62, 2016.

# III

# Development of a Smart Material Actuated Inkjet Printed Robotic Fish

This paper describes the modelling methodology, designing a bi-morph actuated soft robotic fish, manufacturing the actuator samples, assembling it as a system that is operated and tested underwater. Several prototype samples are produced using different substrate material and their usability and performance are tested. My contributions for this paper include modelling, designing the PVDF-based bi-morph actuated robotic fish, assembling the samples as a system and performing all the experiments, processing data, and concluding with the report writing.

# Development of a smart material actuated inkjet printed robotic fish

Keerthi Galagali

***Abstract*—The robotic fishes have the potential to avoid risky underwater work practices, raise safety levels and efficiently swim through complex environments. While several underwater robots are developed in the recent past using smart materials to be more efficient, there is still a huge gap in performance that can be improved. This paper presents a simplified monolithic design of a robotic fish to replace complex designs developed in the past which are bulky and less efficient. A smart material based bi-morph actuator is designed to propel the robotic fish. An inkjet-printed smart material actuated fish is developed such that the PVDF actuator is an integral part of the fish's body. The body of the fish actuates causing the caudal fin to oscillate and generate the wake in water thrust required to propel. The inkjet printing method is successfully implemented by manufacturing uni-morph actuators using PVDF polymer which can be actuated by powering the printed carbon electrodes. The uni-morph actuated robotic fish based on the Novele substrate are found to have an operating frequency of 5.1 $Hz$ when tested in water.**

## I. INTRODUCTION

Nature has been an inspiration to solve several issues in the field of science. Biologically inspired underwater vehicles have the potential to swim through dangerous and dirty environments, collect information, and act according to instructions. In the process of developing underwater vehicles for various applications, several attempts have been made in the past to imitate existing swimming life forms [1], [2]. The underwater robots developed are used for different applications such as—surveillance, defense purpose, an inspection of shipwrecks or underwater equipment, and harvesting energy in oceans [3].

A large share of the research work done in the past deals with locomotion modelling, fluid-structure interactions, hydrodynamics, prototyping and controlling the robotic fish. However, less research has been conducted on developing integrated, monolithic designs using smart materials. The previously developed robotic fish were found to still be bulky, which reduces their efficiency [4]. To overcome this, the objective of the present research is to develop a miniaturized monolithic robotic fish that can mimic the carangiform swimming style to generate thrust and swim efficiently.

This paper fills the gap by designing and developing a smart material actuated inkjet printed robotic fish and evaluating its performance by conducting experiments. This robotic fish is different from the previously developed robotic fish as it has been developed using a PVDF smart material actuator and its swimming locomotion is achieved by actuating the printed electrodes. The printing technology is aimed towards developing individual robots that could also be used in swarms robotics. The research question to be addressed is how to implement PVDF smart material based actuator into a soft robotic fish and make use of deflections achieved by this actuator in propelling the fish.

The paper is structured as follows: In order to design the robotic fish, locomotion modelling is conducted to understand the swimming gait of the fish, as described in chapter II. The robotic fish is designed in such a way as to be able to swim in carangiform mode with a due proportion of undulations and oscillations to be able to maneuver efficiently while achieving speed. Furthermore, a monolithic design of the robotic fish is developed in form of a bi-morph actuator which is detailed in chapter III. The reason for using a bi-morph actuator is that its deformation creates the wake in water required to generate thrust that propels the robotic fish. Although the robotic fish is designed as a bi-morph actuator, the samples manufactured and tested were uni-morph actuators, a decision taken in order to simplify the complexity of the actuator manufacturing process. To realise the underwater robotic fish, several prototype samples of uni-morph actuators are manufactured using the inkjet printing technique as shown in Figure 1. The material choices and manufacturing methodology are detailed in chapter IV. The experiment set-up and experiments conducted to evaluate the performance of the uni-morph actuated PVDF-based robotic fish are explained in chapter V. The results of the experiments are discussed in chapter VI and this paper concludes with a reflection on the research gap addressed in paper-I.

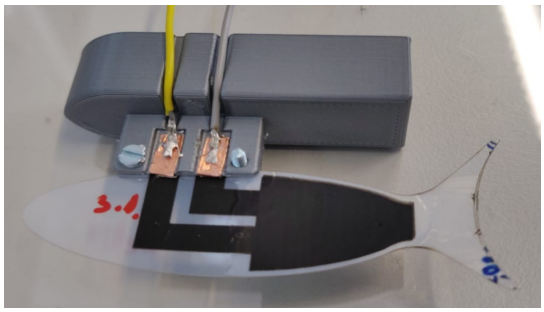

Fig. 1: PVDF-based inkjet printed robotic fish

## II. MODELLING LOCOMOTION OF A SOFT ROBOTIC FISH

Modelling the locomotion of a robotic fish helps in realizing the swimming gait and analyzing parameters that contribute to achieve higher efficiency. The main categories of dynamic models used in the past are: (a) finite elements based models coupled with Computational Fluid Dynamics (CFD) and (b)

simple analytical dynamic models suitable for control and real-time application. In Body caudal fin (BCF) swimming, the thrust is produced solely by body oscillations generated by alternative vortices of a downstream Karman Vortex Stream (KVS). In carangiform mode, a travelling wave increases smoothly from nose to tail of the fish along the longitudinal direction while the propulsive wave travels from nose to the tail.

As the robotic fish to be developed is based on PVDF actuation, it has a compliant body with a certain active actuation region leading to the deflections in the tail. To model the locomotion of the PVDF-based robotic fish, the "hybrid" model proposed by Belkhiri et al. [5] which combines discrete and continuous models taking into account bending and twisting deformations as well as external hydrodynamic forces is one of the well suited models. The algorithms proposed are computationally efficient and this can be used for real-time simulations. It also overcomes modelling deficiencies by considering the fish to be an unconstrained Mobile Multibody System (MMS) based on Newton-Euler (N-E) formulations. This way the exact swimming performance of the robotic fish can be evaluated.

In any locomotion system, the two types of motions experienced are overall rigid motions of degrees of freedom (DOFs) and passive and unactuated motion of internal DOFs. The locomotion of this robotic fish can be modelled mathematically by considering the complaint body as a combination of n segments which are connected by internal joints/links as represented in Figure 2 and whose time variations produce external forces that generate the expected net displacement [6].

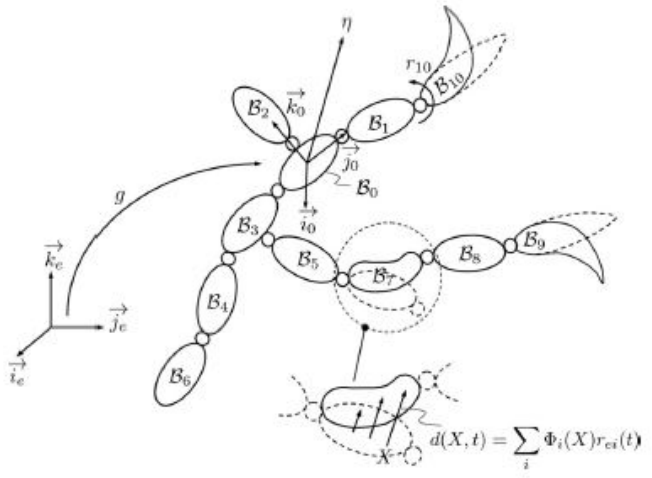


Fig. 2: MMS model with n segments in tree-like structure that is adaptable to model the robotic fish [6]

The distributed flexibility of the robotic fish is modelled in two main approaches: Floating frame approach (FFA) and Geometrically Exact Approach (GEA). FFA is used in order to tackle the deformations and rigid overall motions in a homogeneous way while GEA is used in non-linear structural dynamics. A generalized Newton-Euler model combining FFA and GEA is adopted to solve the dynamics of the robotic fish proposed in [7]. A unique algorithm is used to find the net accelerations based on torque inputs/ joint inputs or reciprocally compute the joint torques when accelerations are provided as an input.

Modelling of the fish's locomotion is done by adapting FFA and GEA with a hybrid algorithm presented in [7] and using recursive iterations. The algorithm deals with forward and inverse dynamics of a soft mobile multibody system (SMMS). The first stage includes forward recursion which evaluates from first joint to the last in order to evaluate the joint velocities. The second stage includes reverse recursion from last join to the first joint evaluating position of the joints using the torque given at each joint. Finally, a forward recursion from first to last is done again to evaluate the net velocity and acceleration.

To simplify the model, initially the algorithm was adapted to a two segment-based system. This would mean that the actuating region of the body is considered as one segment and the tail being the second segment. The displacement achieved with time was evaluated as shown in Figure 3. This model was simplified as there was iterations performed only with respect to time.

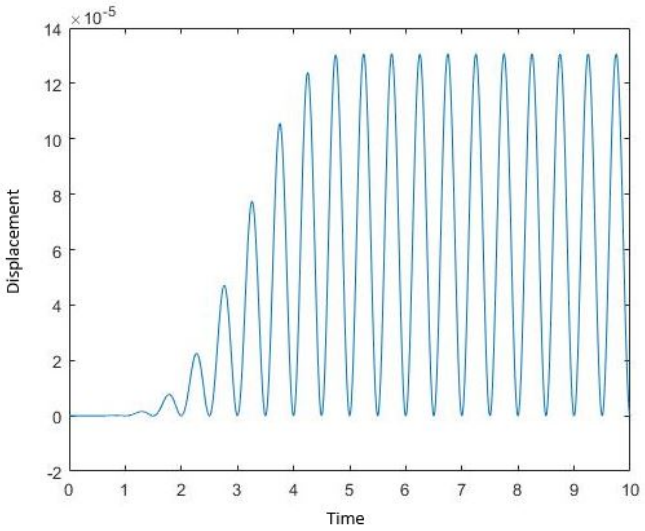


Fig. 3: Simulation results of a 2-segment model

The model was further developed to n-segment system by looping the recursive iterative process described previously. However, the algorithm was not successfully implemented. The major challenges in implementing it to n-segment system was to parameterise the forces generated by actuation of PVDF. The estimation of external forces due to hydrodynamic effect also added to the complexity of evaluating the performance of the robotic fish. Focusing on evaluating the internal torques and external forces acting on each link and their variations with respect to time can help in visualising the change in shape of the fish in real-time. Further, by optimising

the parameters, the actuation force required to achieve certain speed can be estimated aiding to better design of the robotic fish.

## III. DESIGNING THE ROBOTIC FISH

The design of the robotic fish was based on carangiform swimmers. A bimorph actuator was designed in order to have symmetrical deflections of tail oscillations in the lateral direction. The bi-morph actuator was designed with a symmetric electrode-polymer-electrode combination on either side of the substrate as represented in Figure 4. The top and bottom electrodes are positioned in such a way that connectivity can be established between the wires guided by the float and the actuator's electrodes. The polymer PVDF is coated between the electrodes which leads to deflection in the tail when the sample is actuated.

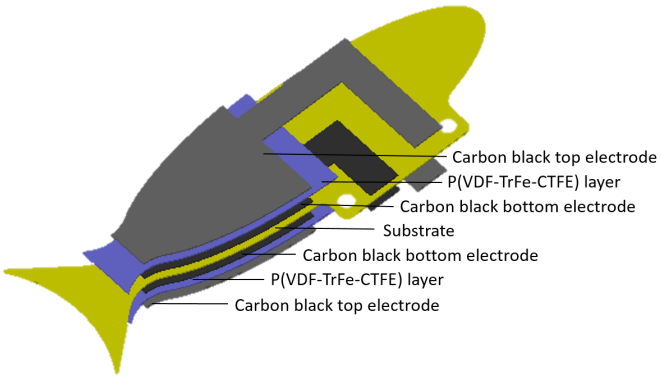


Fig. 4: Schematic representation of a bi-morph actuated robotic fish

The major challenges in designing the robotic fish were miniaturizing the actuator for printing to be both possible and economical, and determining the print region of electrodes and polymer to achieve the range of deflection by the caudal fin to attain the required speed. These parameters could be estimated by modelling. However, as it was not possible, a more practical approach was taken to address some of the main aspects in designing the robotic fish like: overall dimensions, shape imitation (body and fin style), print region used for actuation (both electrodes and polymer), and an additional attachment designed in form of a 'float'.

### A. Size and shape of the robotic fish

Since the inkjet printing technique was used to manufacture the prototype, the overall size of the sample should be in the limits of the print bed size. Since a commercial inkjet printer should be viable to use, the sample size was not supposed to exceed the maximum area of a compact disk (CD) that could be printed. In this case, the maximum possible dimensions of the robotic fish could not exceed $70mm \times 30mm$ as per physical measurements. The overall size of the prototype is thus $60mm \times 20.5mm$. As in carangiform swimmers, one third of the body activates the caudal fin to propel the fish, the print region is from mid-body to the peduncle region and occupies a maximum of $35.5mm \times 18.5mm$ area.

As the shape of the prototype was designed to imitate the shape of a carangiform swimmer, the external shape of the robotic fish was similar to one of them, for example, tuna. It is necessary to understand that due to the divergence of actual specimen, an accurate measurement of the shape of biological fish does not exist and thus cannot be used as a direct input to design a robotic fish. The body of the robotic fish is elliptical in shape, $50mm$ long along the longitudinal axis, and $15mm$ high. The elliptical shape converges with the caudal fin through a narrow necking region in the peduncle [8]. There exist various caudal tail shapes for different functions in fish, the most common once of which are shown in Figure 5. While fast and long distance swimmers have forked and lunate type of tail, short distance and good turning ability can be achieved by swimmers with rounded tail and truncate tail [9]. Because the aim of the present research was to design a fish able to achieve high speed, the lunate tail was chosen for designing the prototype, inspired by that of tuna. The size of the tail was based on dimensional constraints and the aspect ratio that affects the swimming speed [10].

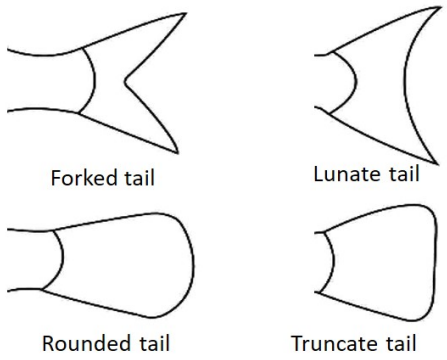


Fig. 5: Caudal fin styles (adapted from [9])

As mentioned in paper I, the active muscle region which actuates the caudal fin of carangiform swimmers occupies about one to two thirds of the body. The printed region of the electrodes and PVDF polymer, which stretches from half of the body until the end of the peduncle region, follows the shape of the fish. The length of the actuation region is $20mm$.

### B. Float design

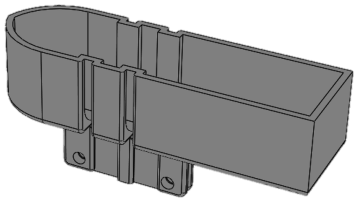

Fig. 6: Design of the float

An attachment to the actuator, which is referred to as 'float', is designed to submerge the robotic fish at a certain depth during experiments. The float was designed to serve two main purposes. One, it should balance buoyant forces with the weight of the actuator, and two, it should have pathways to route the electrical wire connections from the amplifier to the actuator electrodes. The float was designed in the shape of a boat with a nose towards the front to reduce the drag forces, as shown in Figure 6. The float can be attached to the fish on the top via a clamp-like structure using two M2 screws of $5mm$ length each. The float occupies a volume of $2578mm^3$. The weight of the robotic fish was calculated based on the density of the materials used and the volume occupied by each of them. The respective calculations are presented in detail in Appendix A.

## IV. MANUFACTURING

Although bi-morph actuators were designed, only uni-morph actuators were manufactured in order to reduce complexity. This means that the electrodes and the polymer were printed only onto one side of the actuator. The downsides of manufacturing and testing uni-morph actuators instead of bi-morph actuators is that the propelling thrust is reduced due to vortices being generated only one side of the tail and the fish is expected to move in circles instead of forward straight-line propulsion due to asymmetric tail deflections. However, uni-morph actuators can still give an estimate of tail deflection amplitude achievable on one of the lateral sides. The testing of uni-morph actuators will also provide an idea on the performance of the robotic fish to a great extent making it suitable for the present research. This section provides details of the materials used to manufacture the prototype and the process adapted to build the samples. A total of 12 samples were manufactured, as listed in Table I.

| Sample Name | Substrate | Image |
|---|---|---|
| P1 | PEN |  |
| N1 | Novele |  |
| K1 | $25\mu m$ Kapton |  |
| K2 | $50\mu m$ Kapton |  |
| P2 | PEN |  |
| N2 | Novele |  |
| K3 | $25\mu m$ Kapton |  |
| K4 | $50\mu m$ Kapton |  |
| N3 | Novele |  |
| N4 | Novele |  |
| N5 | Novele |  |

TABLE I: A summary of samples produced

### A. Material choice and manufacturing process

To manufacture the prototype samples, four different substrate materials were selected—$50\mu m$ Polyethylene naphthalate (PEN, Goodfellow), polyimide ($25\mu m$ Kapton), polyimide ($50\mu m$ Kapton) and Polyethylene terephthalate (PET) based substrate (Novele IJ-220, Novacentrix). The conductive ink selected for printing the electrodes was carbon black nanoparticle dispersed in ethylene glycol specially formulated to be used with consumer printers (JR-700HV, Novacentrix). These substrate materials and conductive ink were selected because of their better performance on actuators in comparison to other conductive inks with PVDF polymer [11]. The previously developed actuators established a reference and eased the process of manufacturing in-house.

In order to execute the inkjet printing while abiding by the safety norms of nanoparticle exposure in the lab, the inks' safety was assessed, as detailed in Appendix B. To be able to print the electrodes in the desired shape, a PNG file format was generated. The images used for printing are presented in Appendix C. After that, the electrodes were applied by printing repeated layers of carbon black nanoparticle ink, and the electroactive polymer was applied in multiple spin-coated layers. The manufacturing process to develop the inkjet printed uni-morph robotic fish actuator is outlined in Figure 7. However, in order to produce a bi-morph robotic fish actuator, steps 2-7 are to be repeated on the other side of the substrate before cutting the substrate using the laser cutting technique.

Samples P1, K1, K2 and N1 were the first set of robotic fish samples manufactured so that the print could be tested on PEN, Kapton $25umm$, Kapton $50umm$ and Novele respectively. These samples did not have the capacity to undergo experiments as they were test samples created to check the quality of the print on them. However, the other samples listed in Table I followed the procedure as depicted in Figure 7 to undergo tests described in the next section.

### B. Assembly

The floats to be attached to the actuator samples were manufactured with the 3D printing technique using PLA material in Prusa printers. The inkjet printed actuators were

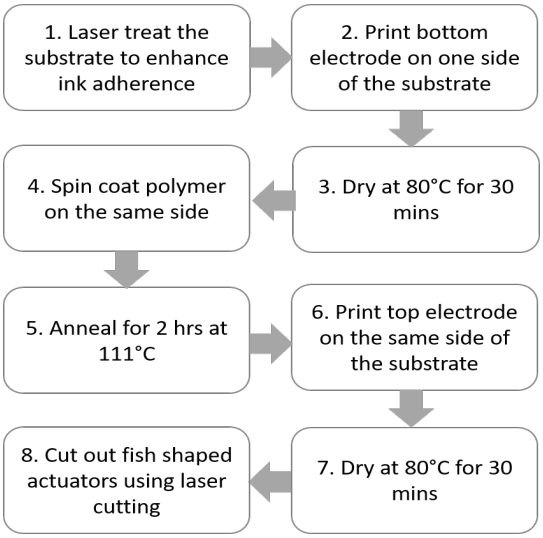


Fig. 7: Manufacturing steps for producing inkjet printed unimorph actuators

then glued to adhesive copper tape using a conductive glue before being attaching them to the float. The copper tape adheres to the float's routing pathway on one end and to the actuator's electrode on the other end. The electrical connection was established by soldering wires onto the copper tape as seen in Figure 8.

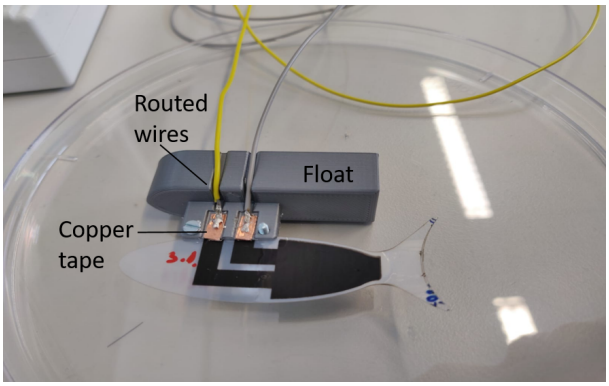


Fig. 8: Actuator attached to the float with established electrical connections

## V. EXPERIMENTS

As mentioned previously, different versions of the robotic fish were developed using four different types of substrate. Three sets of experiments were conducted on these actuators. The first set of experiments was conducted to test the behaviour of the substrate material when coated with silicone to turn the actuator into a water-proof system. Silicone has been previously used in building an underwater robot as seen in [12]. The second set of experiments was conducted to evaluate the operating frequency of the actuator under different conditions at which it produces a maximum deflection in the fish's tail. The third set of experiments were conducted to check the performance of the fish and evaluate its velocity when actuated in a fish tank.

### A. *Water-proof coating test*

In the first set, actuator samples P1, N1, K1 and K2 which are made from four different substrate materials were coated with silicone (Ecoflex 00-10) and cured as shown in Figure 9 to turn the actuators into a water-proof system. Ecoflex 00-10 was chosen as the material to make the system water-proof, because it has the properties of being very strong and stretchy after curing. It could also be cured at room temperature within four hours. The goal of this experiment was to identify how the material's stiffness affects the curing process of the silicone coating.

(a) Kapton $25umm$

(b) Kapton $50umm$

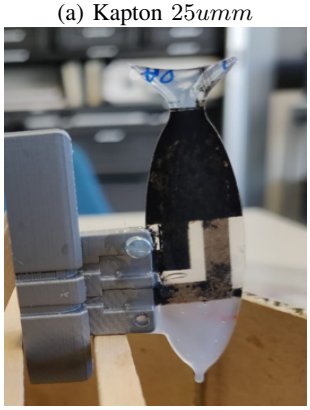

(c) Novele

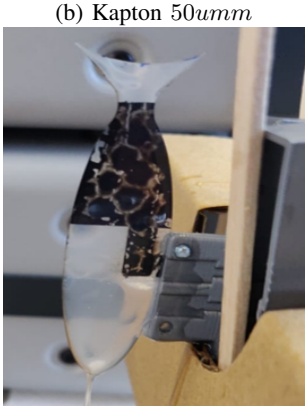

(d) PEN

Fig. 9: Substrate samples tested by dipping them in silicone

If the material is flimsy, i.e., not stiff enough, deflections might develop during the curing process, which will lead to induced stresses. It was noticed that samples K1 and K2 were drooping as the material was not stiff enough. This caused the silicone to drain unevenly during the curing process. Thus, the samples K3 and K4 were laser cut in a different shape as seen in Table I to spin-coat silicone while resting the samples in horizontal direction on a mould instead of a regular silicone dip. However, samples P1 and N1 were found to be sturdy enough during the curing process and hence the other samples made from PEN and Novele substrates were dipped and cured in a regular fashion.

### B. Operating frequency identification test

In the second set, a total of three experiments was conducted on samples P2-N5, as listed in Table I: an operating frequency identification test in air *without* waterproof coating, an operating frequency identification test in air *with* waterproof coating, and an operating frequency identification test in water. The operating frequency is determined based on maximum tail deflections observed when the sample is actuated at resonance frequency. The experimental setup for all the three experiments is similar, with only a few minor alterations that will be explicitly mentioned. The experiments were conducted in order to identify the operating frequency in various conditions.

*1) Experiment set-up:* The setup consists of a Lenovo Thinkpad E470 with NI LabVIEW 2018, a high voltage amplifier (MFC 1500/50, Smart Materials), a laser distance sensor (ILD1750-2, Micro-Epsilon) and a data acquisition system (NI USB-6211) as depicted in Figure 10a. The actuator and laser triangulation sensor were contained inside a clear acrylic chamber to isolate the system from external disturbances or air flow, as well as to keep all electrical contacts isolated for safety purposes as seen in Figure 10b. Furthermore, in all three experiments, the actuator is clamped horizontally and placed below the laser triangulation sensor such that the amplitude of the actuator's tail deflection can be determined.

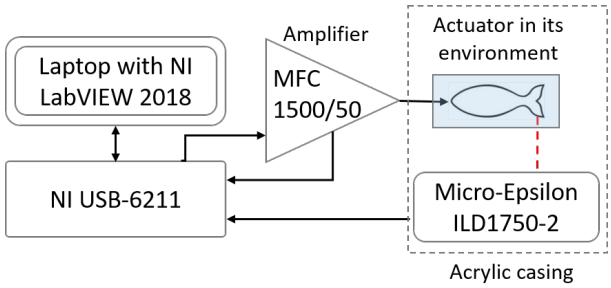


(a) Schematic representation

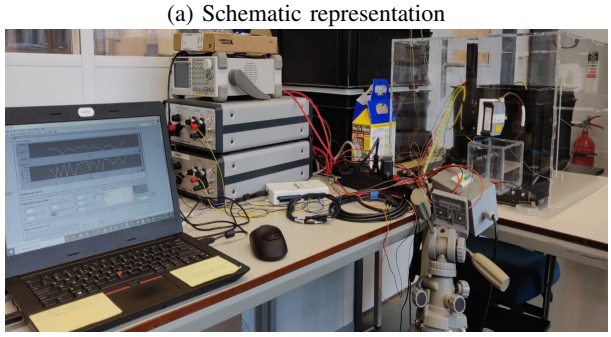

(b) Actual experimental set-up

Fig. 10: Set-up for operating frequency evaluation test

*2) Operating frequency identification test without silicone coating in air:* The physical set-up for the first experiment, i.e., the operating frequency identification test in air without silicone coating, is shown in Figure 11. The first experiment is aimed at obtaining the operational frequency of the designed actuator. The operational frequency of the actuator is chosen to be the frequency of the generated signal that produces the maximum amplitude of the tail deflection during actuation. The performance of the actuator samples in this experiment confirms that there are no defects in the manufacturing process.

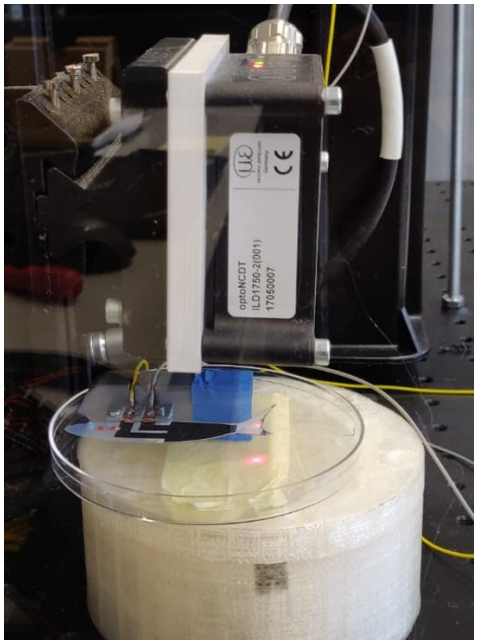

Fig. 11: Actuator being tested in air to evaluate operating frequency

To obtain the operational frequency, a chirp signal is generated using the LabVIEW program. The generated signal is amplified using the high voltage amplifier. The amplified signal is then fed to the actuator's electrodes. The actuation results in tail deflection, the amplitude of which is measured using the laser triangulation sensor. The National Instruments data acquisition system (NI DAQ system) is used to document the signal generated using LabVIEW, the amplified signal, and the amplitude of the tail deflection. The data is then fed back to the laptop and saved for further analysis.

*3) Operating frequency identification test with silicone coating in air:* The physical set-up and procedure for the second experiment was identical to the first experiment, except that in the second experiment the actuator was coated with silicone rubber (Ecoflex 00-10) turning the actuator into a waterproof system. This experiment was conducted to examine the effect of silicone coating on the actuator's performance in tail deflection. It is expected that the resonance frequency of the actuator sample reduces in comparison to previous experiment as there is an addition of mass to the system.

*4) Operating frequency identification test with silicone coating in water:* The third experiment was conducted to evaluate the operating frequency in water. The physical set-up used for this experiment is shown in Figure 12. The set-up and the procedure for the third experiment were identical to the first and second experiment, except that the actuator coated with silicone was now fully submerged in water. This test was conducted to examine the deflections attained by

the actuators in water and the effect of hydrodynamics on the shape and material of the actuator used. The operating frequency is expected to reduce further when operated in water and the magnitude of the deflection achieved by the tail also reduces due to the dampening effect from the surroundings. The samples were actuated at different voltage amplitudes to test the maximum deflection amplitude attained in each of the three operating frequency identification experiments mentioned above.

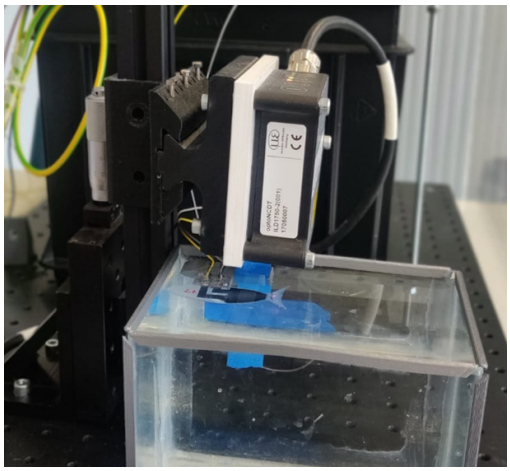

Fig. 12: Experiment set-up to evaluate the operating frequency in water

### C. Performance evaluation of the robotic fish

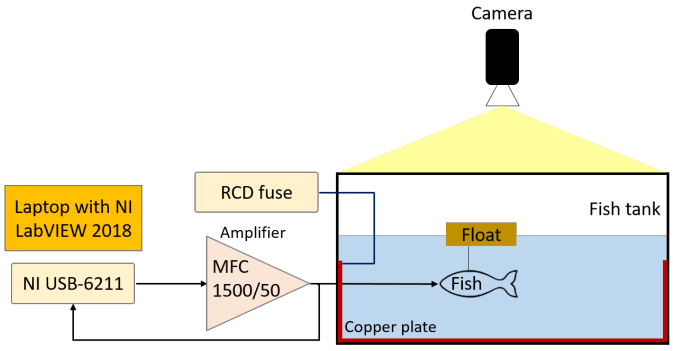


Fig. 13: Experiment set-up to evaluate the performance of the robotic fish

The schematics for the final experiment are depicted in Figure 13. It consist of a Lenovo thinkpad E470 with NI LabVIEW 2018 (used to generate the sinusoidal signal used for actuation), the NI DAQ system, a high voltage amplifier, a fish tank with copper plate immersed in water to extract any residual current from leakage connected to a Residual-current device (RCD) fuse for safety purpose and a hand-held camera to record the performance of the fish. The set-up is similar to operating identification experiments except that the laser triangulation sensor is replaced with a hand-held camera and the sample is not clamped anymore but is dropped freely in the fish tank. The actual set-up is thus same as shown in Figure 10b.

The input sinusoidal signal to the amplifier was operated at the frequency identified in the operating frequency identification test in water which was found previously. The voltage amplitude of the signal was chosen such as not to cross the break-down voltage of the material. The amplified signal was then fed to the actuator via the wires routed on the float. A mobile camera was placed over the fish tank to capture the movement of the fish. The recorded motion of the fish could then be analysed by manually tracking the tail position using manual tracking method as presented in the MATLAB code in Appendix D. This performance test was conducted by releasing the robotic fish assembly in a fish tank to evaluate the performance of the fish. As the robotic fishes were actuated using uni-morph actuators, the fishes were not expected to swim in a straight line but in circular pattern as tail deflections were asymmetrical.

## VI. RESULTS AND DISCUSSIONS

A soft robotic fish in form of a bi-morph actuator was designed as detailed in chapter III to meet the design requirements. Furthermore, the actuator samples listed in Table I were manufactured according to the methodology described in Figure 7, using four different types of substrates, namely —PEN, $25\mu m$ Kapton and $50\mu m$ Kapton and Novele. While samples P1, N1, K1 and K2 were printed for testing the ink deposition on the substrate material, samples P2, N2, K3, K4, N3, N4 and N5 were tested to examine the feasibility of using inkjet printed actuators as underwater robotic fish and their behaviour towards actuation is tested in different environments as described in chapter V. The results of the operating frequency identification experiments and performance test of different samples tested are listed below.

### A. Operating frequency identification test results

The samples tested to evaluate their operating frequency were actuated under three set-ups as mentioned in chapter V. The tail deflections recorded by the laser triangulation sensor for each of the samples were processed to evaluate the frequency response of the system.

*1) P2 sample results:* Figure 14 shows the frequency response of sample P2. Image (a) depicts the results when the sample is actuated at 100V before coating it with silicone. The operating frequency is found to be at $17.3Hz$. Image (b) depicts the response when actuated at 180V while the operating frequency observed after coating it with silicone is $7.3Hz$. It is difficult to point the exact operating frequency when operated under water. In image (c), the operating frequency when actuated in water is found to be between $1Hz$ to $2Hz$.

*2) N2 sample results:* Figure 15 shows the frequency response of sample N2. Image (a) depicts the results when the sample is actuated at 150V before coating it with silicone and the operating frequency is found to be at $37.6Hz$. Image (b) depicts the response when actuated at 180V while the operating frequency observed after coating it with silicone is

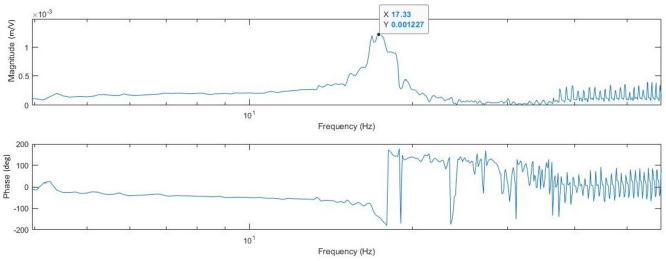


(a) Frequency response of P2 without coating in air

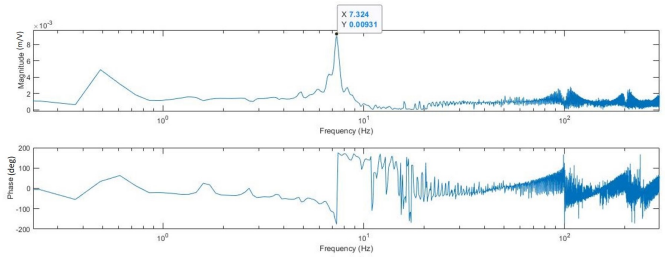


(b) Frequency response of P2 with silicone coating in air

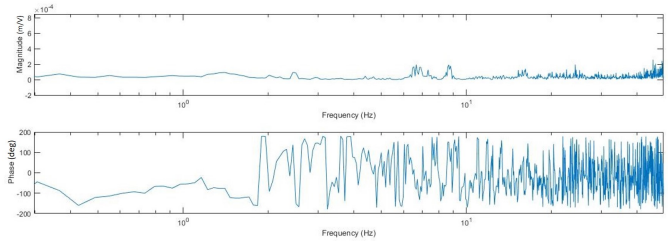


(c) Frequency response of P2 with silicone coating in water

Fig. 14: Response of P2 sample when tested for the operating frequency

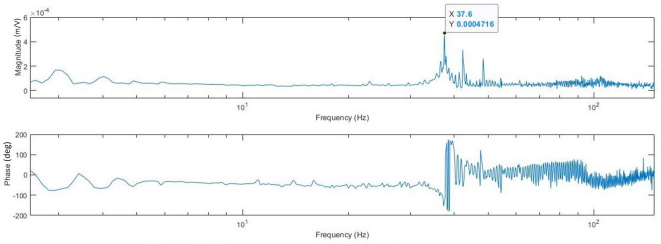


(a) Frequency response of N2 without coating in air

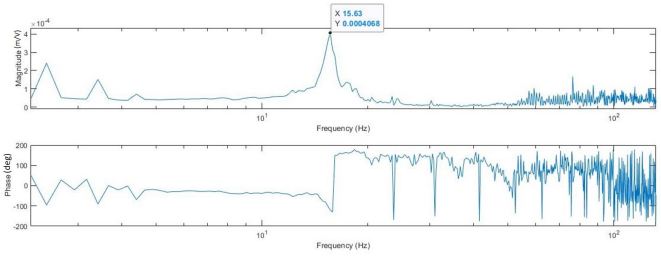


(b) Frequency response of N2 with silicone coating in air

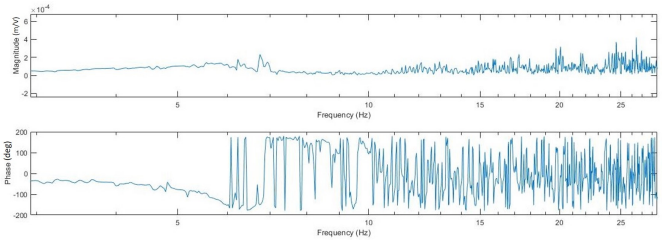


(c) Frequency response of N2 with silicone coating in water

Fig. 15: Response of N2 sample when tested for the operating frequency

15.6$Hz$. The operating frequency when actuated in water is found to between 6$Hz$ to 7$Hz$ as seen in image (c).

*3) K3 sample results:* Figure 16 shows the operating frequency of the sample after coating it with silicone is at 3.8$Hz$. However, the coherence for this sample was not good. This sample could not be tested for operating frequency before coating it with silicone to test if the actuator works because this sample was made of 25$\mu m$ Kapton which has a very low material stiffness, making silicone coating by regular dipping difficult. In that case, the design was altered to suit the spin coating technique to coat the silicone.

It was observed that this sample had the least stiffness in comparison to other samples and the tail part of the sample drooped under its own weight while undergoing the test to evaluate the operating frequency in air. The force generated by the actuator was not sufficient to overcome self-weight resulting in low coherence when tested as seen in Figure 16 between 1$Hz$ to 4$Hz$. While testing the sample underwater, it was noticed that the self-weight and the hydrodynamic forces around the sample made it difficult for any tail deflections to be recorded.

*4) K4 sample results:* Due to the reason explained in the previous section, the operating frequency of this sample could also not be recorded before coating silicone. K4 was thus

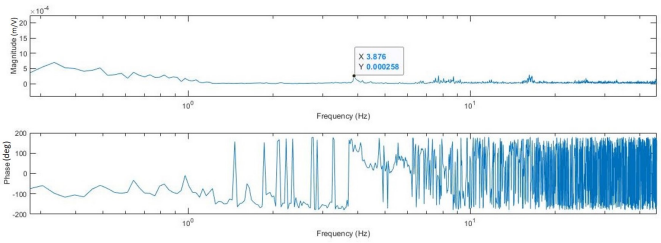


Fig. 16: Response of K3 sample when tested for the operating frequency in air with silicone coating

also designed to undergo silicone coating by the spin coat technique. Figure 17 shows that the operating frequency of the sample when tested in air after coating it with silicone is at 8.9$Hz$, while the operating frequency observed under water is not clear due to heavy dampening and low coherence observed while conducting the experiments.

*5) N3 sample results:* Figure 18 shows that the operating frequency of the sample before coating it with silicone is at 39.3$Hz$, while the operating frequency observed after coating it with silicone is 21.8$Hz$. The operating frequency for the sample when tested in water was found to be at 5.1$Hz$.

*6) N4 sample results:* Figure 19 shows that the operating frequency of the sample before coating it with silicone is at

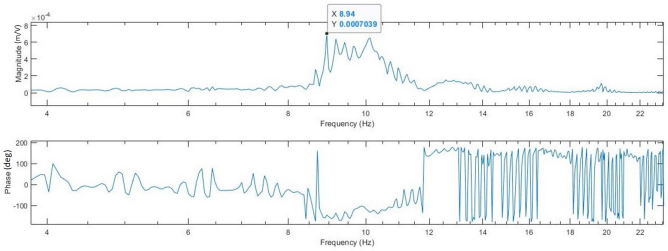


(a) Frequency response of K4 with silicone coating in air

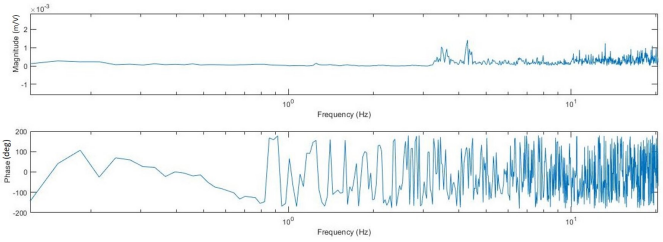


(b) Frequency response of K4 with silicone coating in water

Fig. 17: Response of K4 sample when tested for the operating frequency

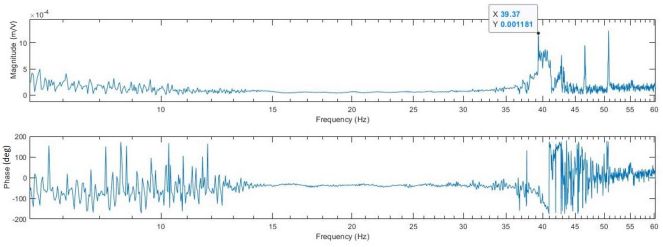


(a) Frequency response of N3 without coating in air

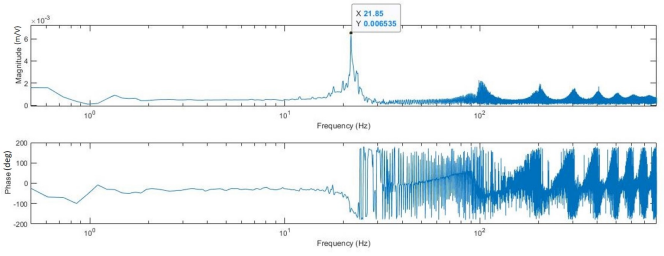


(b) Frequency response of N3 with silicone coating in air

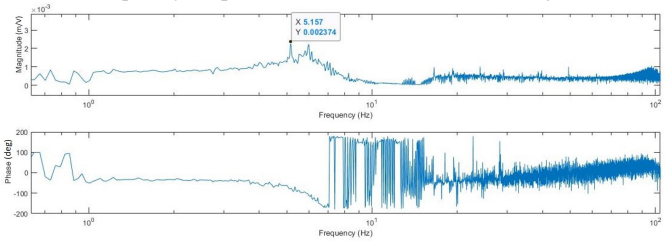


(c) Frequency response of N3 with silicone coating in water

Fig. 18: Response of N3 sample when tested for the operating frequency

31.5$Hz$, while the operating frequency observed after coating it with silicone is 29.9$Hz$. The operating frequency when

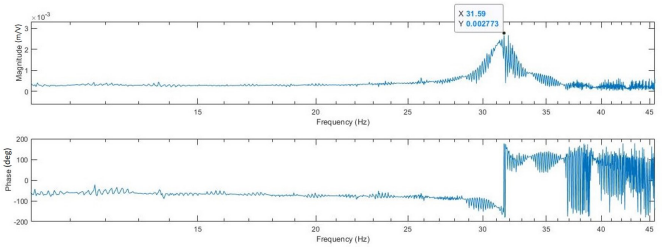


(a) Frequency response of N4 without coating in air

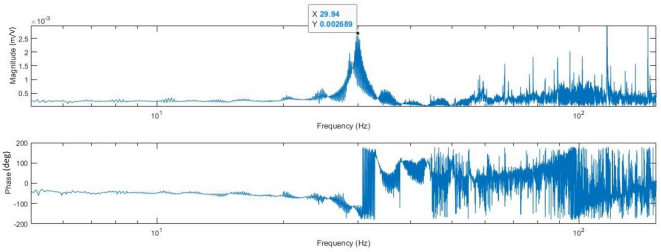


(b) Frequency response of N4 with silicone coating in air

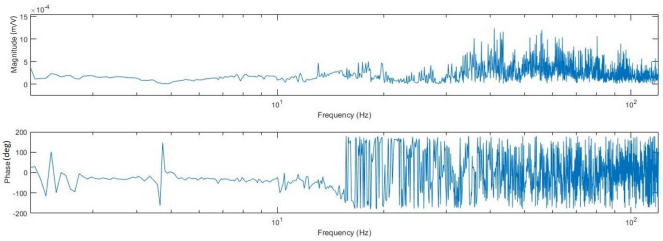


(c) Frequency response of N4 with silicone coating in water

Fig. 19: Response of N4 sample when tested for the operating frequency

tested underwater was hard to determine, however, based on the change of phase, an estimate can be made that the operating frequency is between 10-20$Hz$ as seen in image (c).

*7) N5 sample results:* Figure 20 shows that the operating frequency of the sample before coating it with silicone is at 31.6$Hz$, while the operating frequency observed after coating it with silicone is 21.6$Hz$. This sample underwent a failure while testing for operating frequency in air as its silicone coating was broken. It was then re-coated with silicone to test whether it functions, which it did, as shown in Figure 20 (b). However, due to the faulty re-coating, the silicone broke down while testing the sample in water, leading to a short-circuit in the sample. Fumes from the sample electrode region were noticed when it underwent actuation.

### *B. Performance evaluation results*

Post testing the samples for identifying the operating frequency in order to achieve maximum displacement in the caudal fin, final performance test was conducted. Several samples had failed to reach this stage of experimentation due to several possible reasons listed in the next section under discussions. The only samples that were able to undergo performance test as described in the last part of experiments

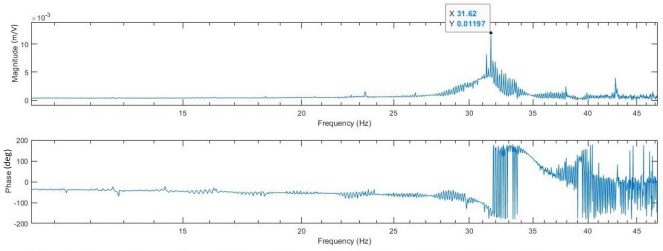


(a) Frequency response of N5 without coating in air

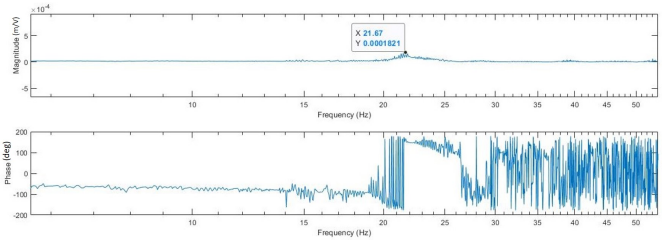


(b) Frequency response of N5 with silicone coating in air

Fig. 20: Response of N5 sample when tested for the operating frequency

section were N3 and N4. The samples were tested in a fish tank to check their performance as depicted in Figure 13. However, N4 also fumed up when operated in the water as the electrical connectivity was not established in a successful way. Sample N3 was operated at $5Hz$ (operating frequency identified when tested underwater) with different input voltages to test its performance. The displacement of water in the tank was noticeable when sample N3 was operated at 180V and $5Hz$ , but there was no net propulsion observed.

### C. Discussions

*1) Manufacturing:* During the manufacturing of the samples, the substrate material, the number of layers printed to build the electrodes and polymer coating between the electrodes played a key role. As pointed out in the previous section, the sample N5's silicone coating ripped apart and had to be re-coated before testing it again. However, as the print layers of the electrode was good, even though the first layer of print was damaged, the sample worked when it was tested again. This shows the importance of print quality while manufacturing the samples.

Based on the material of the substrate used, it can be noticed that $25\mu m$ Kapton and $50\mu m$ Kapton were the least feasible substrate due to their material stiffness properties. Their low stiffness resulted in drooping of the substrate under their own weight. This was overcome by spin-coating the Kapton substrate samples. This helped in improving the silicone coating process but however did not help in improving the performance of the samples.

The assembly of the samples with the 3D printed float was crucial as well to establish good electrical connectivity between actuator's electrodes and the wires routed on the float. Any error in the connectivity could lead to short-circuit in the sample. The procedure of coating the fish with the silicone had to done carefully to ensure that the coating was evenly distributed around the sample and no deformations were caused while the silicone drained from the samples during the curing process.

*2) Errors due to water-proofing:* Sample P2 and N2 were fumed up while being tested for the operating frequency under water. This happened due the defect in silicone coating. The float was not completely coated to turn the system water-proof. This allowed water to enter into the sample through capillary action and caused the failure of the prototype samples. The swelling of the prototype sample can be seen in Figure 21. A comparison evidently shows that the water seepage led to failure of the sample as seen in Figure 22.

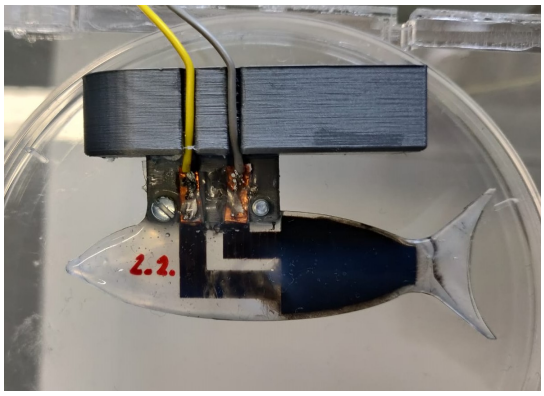


Fig. 21: Swelling observed in sample N2

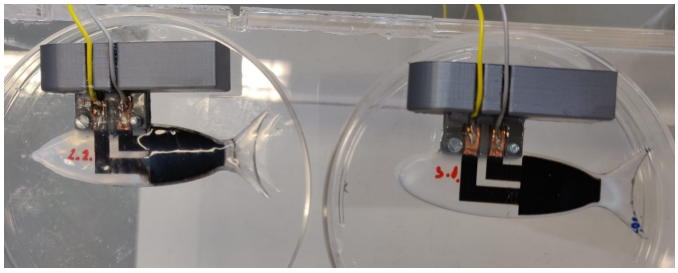


Fig. 22: Comparison of samples N2 and N3 after being tested in water

Samples K3and K4 faced issues with regular silicone dipping process as described earlier. Thus, K3 and K4 had to be adopted to spin coating technique instead of regular silicone dip. These samples were cured in the moulds that they were spin coated in.

Silicone coating of sample N5 was ripped apart after being tested for operating frequency in air as the solder was not coated well. It was noticed that the ink deposited on the top electrode was also scrapped off as the silicone coating was removed. However, an attempt was made to re-coat the sample with silicone to test it again for the operating frequency. The result of operating frequency recorded in the air before the damage of the silicone coating and post re-coating the sample

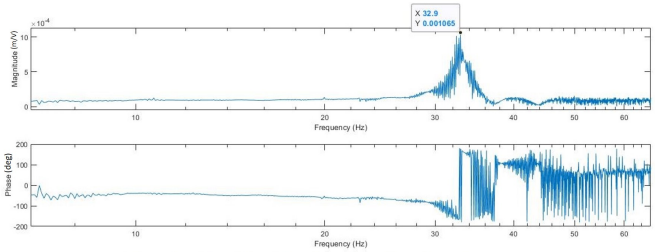


(a) Operating frequency recorded after first coating

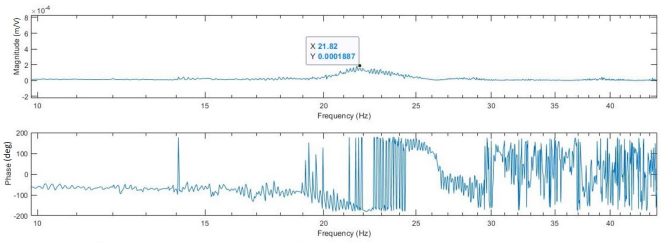


(b) Operating frequency recorded after second coating

Fig. 23: Difference in the operating frequency recorded before and after re-coating N5 with silicone

is depicted in Figure 23. A shift of frequency is observed from $32.9Hz$ to $21.8Hz$ with a significant drop in the magnitude.

*3) Operating frequency identification test:* A trend of the operating frequency reducing when the samples are tested in air with silicone coating in comparison to without silicone coating is observed due to the added stiffness. A further reduction in the operating frequency is observed when tested in water with reduced deflections due to increased stiffness and dampening effect from the surrounding.

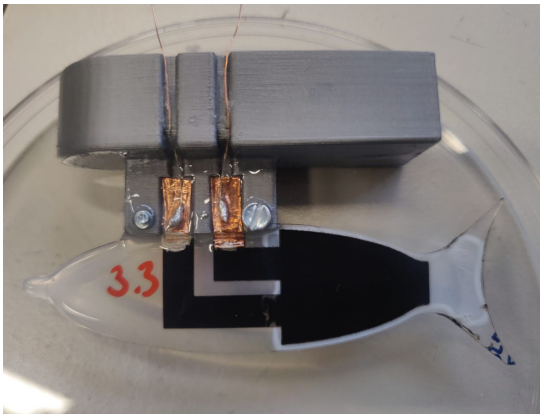


Fig. 24: Altered copper wiring routed onto the float

*4) Performance evaluation:* During this test, it was noticed that the wires connected to the actuators were too stiff leading to increased resisting force. The weight of the wires contributed to the resisting forces apart from the drag forces. To overcome these shortcomings, the wires were then changed to copper wires of lower stiffness and weight as shown in Figure 24.

The float was designed for a bi-morph design, however, using the same for a uni-morph design caused an imbalance in the robotic fish's center of gravity as the print and the electrical connections were made only on one side of the float making it lean inwards on the printed side. The uneven silicone coating added further to the imbalance making it difficult for the tail to move as expected. The deflection produced by the tail of the fish was observable due to ripples in the water at the operated frequency. However, the deflections were not large enough to propel the fish.

## VII. CONCLUSIONS

In this paper, the concept of a bi-morph actuator integrated into a robotic fish to imitate carangiform swimming style is designed. The robotic fish samples are manufactured using the inkjet printing technique by printing the electrodes to actuate PVDF based smart material. Uni-morph actuators are manufactured using four types of substrate materials to test the concept and were found operational when tested in water. The operating frequency of the samples reduce when tested with silicone coating in comparison to without silicone coating and even further when tested in the water as expected due to increased stiffness. The operating frequency for the sample made of Novele substrate when operated in the water is found to be at $5.1Hz$ for N3 sample. The performance of the fish sample N3 was observed proving the implementation PVDF actuation underwater successful. With some improvements in modelling, actuation region design can be optimised. Further, manufacturing bi-morph actuators could prove the feasibility of developing an autonomous robotic fish.

## REFERENCES

[1] A. Raj and A. Thakur, "Fish-inspired robots: design, sensing, actuation, and autonomy—a review of research," *Bioinspiration & biomimetics*, vol. 11, no. 3, p. 031001, 2016.

[2] A. A. M. Faudzi, M. R. M. Razif, N. A. M. Nordin, E. Natarajan, and O. Yaakob, "A review on development of robotic fish," *Journal of Transport System Engineering*, vol. 1, no. 1, pp. 12–22, 2014.

[3] "12-cutting-edge-technologies-that-could-save-our-oceans," https://www.weforum.org/agenda/2016/09/12-cutting-edge-technologies-that-could-save-our-oceans/, Accessed: 2020-11-07.

[4] W.-S. Chu, K.-T. Lee, S.-H. Song, M.-W. Han, J.-Y. Lee, H.-S. Kim, M.-S. Kim, Y.-J. Park, K.-J. Cho, and S.-H. Ahn, "Review of biomimetic underwater robots using smart actuators," *International journal of precision engineering and manufacturing*, vol. 13, no. 7, pp. 1281–1292, 2012.

[5] A. Belkhiri, M. Porez, and F. Boyer, "A hybrid dynamic model of an insect-like mav with soft wings," in *2012 IEEE International Conference on Robotics and Biomimetics (ROBIO)*. IEEE, 2012, pp. 108–115.

[6] F. Boyer and A. Belkhiri, "Reduced locomotion dynamics with passive internal dofs: Application to nonholonomic and soft robotics," *IEEE Transactions on Robotics*, vol. 30, no. 3, pp. 578–592, 2014.

[7] F. Boyer, M. Porez, F. Morsli, and Y. Morel, "Locomotion dynamics for bio-inspired robots with soft appendages: Application to flapping flight and passive swimming," *Journal of Nonlinear Science*, vol. 27, no. 4, pp. 1121–1154, 2017.

[8] J. Yu and M. Tan, *Motion Control of Biomimetic Swimming Robots*. Springer, 2020.

[9] "Nature's unifying patterns," https://toolbox.biomimicry.org/core-concepts/natures-unifying-patterns/shape/, Accessed: 2020-11-07.

[10] V. C. Sambilay Jr *et al.*, "Interrelationships between swimming speed, caudal fin aspect ratio and body length of fishes," *Fishbyte*, vol. 8, no. 3, pp. 16–20, 1990.

[11] K. Baelz, "P(VDF-TrFe-CTFE) actuators with inkjet printed electrodes," 2019.
[12] T. Li, G. Li, Y. Liang, T. Cheng, J. Dai, X. Yang, B. Liu, Z. Zeng, Z. Huang, Y. Luo *et al.*, "Fast-moving soft electronic fish," *Science Advances*, vol. 3, no. 4, p. e1602045, 2017.

# IV

# Conclusions

This thesis work dealt with developing an inkjet printed smart material actuated robotic fish. With two-thirds of our earth covered by water, there are several activities executed on a daily basis underwater [1], [2], [3], [4]. However, there are risk and safety concerns associated which could be reduced by developing efficient and agile underwater robots [7]. The initial study indicated that the smart material-based robotic fishes have not been explored in all dimensions and there is a need to develop a more efficient robotic fish when compared to the existing ones. The objective of this work was to develop a compact monolithic based design to drive the robotic fish efficiently.

During the initial research stage, it was found that mimicking fish has many aspects to be looked into. The most important ones were- designing the fish to mimic a particular swimming style, deciding on the type of actuation and then choosing the material to achieve necessary actuation, studying modelling techniques to imitate the swimming gait, understanding manufacturing techniques and experimental methods. It was evident that among the different swimming styles, carangiform of BCF style was effective with respect to both efficiency and maneuverability. The trend of actuation was observed to shift from motor-operated robotic fishes to that of smart material actuated robotic fishes in the recent past to reduce the complexity and bulkiness of the underwater robots. Among smart actuators, EAP based IPMC actuators and SMAs were most commonly used. A potential material PVDF based actuator developed in-house at TU Delft was found suitable as well. Manufacturing PVDF based actuators were found feasible in-house. Lastly, modelling techniques to mimic the swimming gait were studied to see the feasibility of using one of them to model the robotic fish to be developed. The literature study showcased several possibilities and paths that could be taken to develop better robotic fish.

The second paper demonstrates the implementation of PVDF based actuation to propel the robotic fish. A modelling technique was adapted accordingly to be able to mimic the continuity in the actuation and movement of the swimming gait by using a hybrid algorithm [6]. The algorithm disintegrated the body of the fish into 'n' segments to build a continuous system that would be acted upon by torques at the joints between the segments leading to the net displacements of the robotic fish. The robotic fish was designed as a bi-morph monolithic actuator based on carangiform swimmers to be able to produce symmetric tail deflections in the lateral direction. With one-third of the body actuating the tail, the overall size of the robotic fish was $60mm$x$20.5mm$. To manufacture and test the performance of the actuator, uni-morph actuators were produced based on four different substrates- PEN, $25\mu m$ Kapton, $50\mu m$ Kapton, and Novele. These actuators were tested initially to observe their behavior when coated with silicone. It was observed that PEN and Novele substrates which were stiffer could be dipped directly and cured, but Kapton substrate required support while curing due to their lower stiffness. As the performance of the actuator samples would be affected by actuator properties, water-proof coating, and the surrounding environment (air/water), the samples produced were characterized by three different experiments. The samples were tested for their operating frequency in the air before coating them with silicone, then they were tested after coating them with silicone in air, and finally in the water. Samples built on PEN and Novele substrate performed better than those built on Kapton

substrate. PEN substrate recorded highest tail deflections at $17Hz$ in the air before being coated with silicone while its resonance frequency reduced to $7.3Hz$ after coating and it further reduced to around $1.5Hz$ when tested in the water due to the dampening effect. Novele substrate recorded highest tail deflections at $31Hz$ before silicone coating while it reduced to $21Hz$ in the air after coating and further reduced to $5.1Hz$ in water. Among PEN and Novele substrates, Novele substrate performed better by producing deflections of 0.002m in water. In the final experiment, the samples were tested to swim freely in the water. However, there was no net displacement observed.

This project has successfully implemented a PVDF-based actuator in developing an underwater robotic fish. To improve the performance of the fish, the overall system design has to be optimized such that the tail deflections can propel the robotic fish. It can be achieved by modelling the fish efficiently and manufacturing bi-morph actuators as recommended in the next section.

# V

# Reflections and Recommendations

This thesis project included various aspects of development of a robotic fish. Each step towards the realization of the robotic fish posed challenges as listed below.

- The current state of the art had no references to soft robots manufactured by an inkjet printing technique. Most robots previously developed used SMAs [13], IPMC [16], [14], or other piezo-based EAP [18]. These robots used other manufacturing techniques to develop the robot, leading to a lack of references.
- The modelling posed challenges as the adaptation of the hybrid algorithm mentioned in paper II for a multi-linked robot was not easy. The extension from a 2-link robot to that of a multi-link required a deeper understanding of the algorithm to be able to optimize the dynamics of the fish.
- The chosen swimming style —carangiform required one-third to a two-thirds portion of the robotic fish body to actuate the tail [17]. The actuator's design was based on this requirement. However, the activation region has not been optimised as the modelling was not completely implemented.
- Several iterations were required before a suitable bi-morph actuator could be designed. The details such as dimensions, shape, body and tail design, and active actuation region were based on several adaptations from previously designed underwater robots and limitations within this project.
- The manufacturing suffered a delay in deliveries of the experimental set due to the COVID-19 pandemic. There were other challenges with respect to assembling the manufactured actuator samples with other entities used in the experiment like handling the thin substrate material, making the robotic fish a water-proof system, and connecting cables to successfully establish electrical connectivity.
- The experimentation phase was crucial and critical. Several experimental set-ups were studied before performing experiments for the actuator samples manufactured [18], [9]. The method of testing the samples for each experiment was compared to experimental set-up described in the literature. Each sample was tested and analysed under different conditions to improve the next prototype sample to overcome shortcomings noticed in the previous experiments.

With several aspects involved in this project, it can be improved in different dimensions by the following future work.

- Modelling technique described in the paper II can be adapted and used to improve the design of the fish. The hybrid algorithm could be used to develop an efficient robotic fish by optimising the parameters involved in the design.

- The design of the fish can be improved to optimise the actuation region to implement carangiform swimming.
- Manufacturing bi-morph actuators could be challenging. If executed successfully, the robotic fish samples could swim along a straight path. Printing of bi-morph actuators however would require training to avoid the carbon particles deposited on one side of the actuator from being damaged while printing the other side.
- While conducting the experiments, the system can perform better if wires with lower stiffness are used to supply the power such that they do not hinder the propulsion. It would be better if the circuit could be printed on the surface with an on-board power supply system. However, this is a very far fetched idea.
- The silicone coating can be applied by spin coating for all substrates to generate evenly distributed thinner walls. It is essential to take care that the system is completely sealed to avoid any leakage of water into the system to avoid short-circuit.

By implementing the above suggestions, an efficient robotic fish can be developed when compared to the ones seen in the literature.

# A

# Float Design

The float design underwent multiple iterations and was designed to balance the buoyant forces in the direction of gravity to counter the robotic fish's weight. It was shaped in form of a boat with lesser width when compared to its length to reduce the drag forces. The robotic fish was initially designed with electrodes as shown in Figure A.1a. Although the print area of the electrodes remained the same, the electrode contact points were altered to extending the paths of the ends to be able to connect to the float attached on the top as seen in paper II. The front of the float was shaped like a nose to further provide an aerodynamic effect to reduce the drag forces. Figure A.1 represents the iterations undergone before the final float was designed as seen in Figure A.1d.

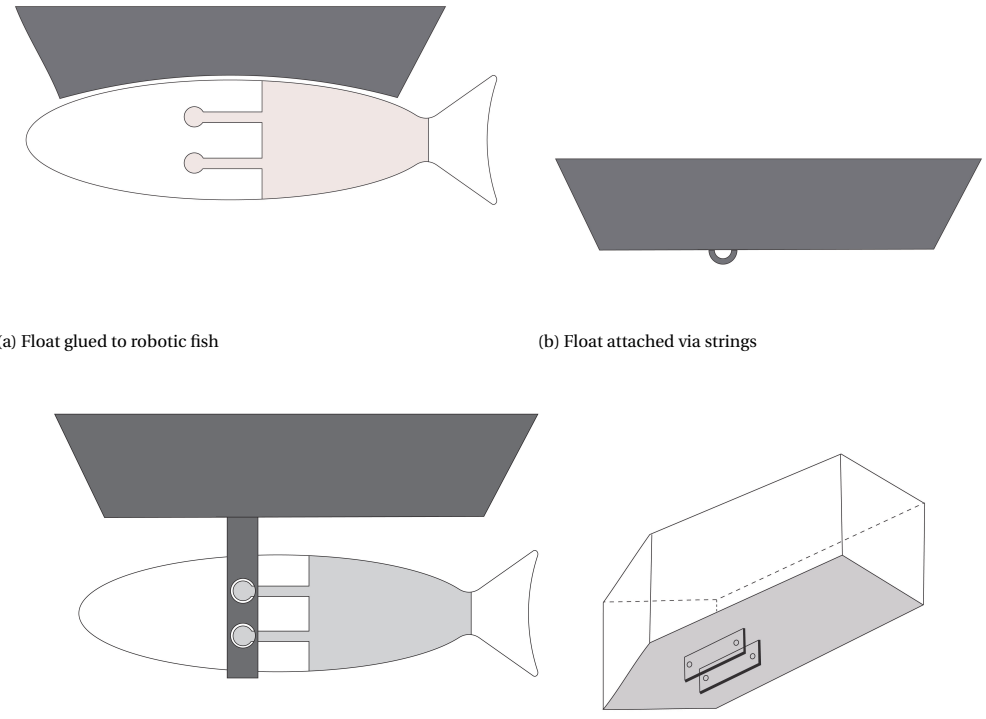

(a) Float glued to robotic fish

(b) Float attached via strings

(c) Float clamped around the fish

(d) Float with screw facility

Figure A.1: Different float designs tried and tested to balance the buoyant forces

The first idea was to attach the float by gluing it directly onto the fish. However, since the area of attachment would then be very minimal, the second iteration of attaching the float via a string hooked on one end to the float and on the other end to the robotic fish was thought of. This would generate buoyant force but would not allow stability in the horizontal direction for thrust to be utilized to the maximum extent. The third idea was to clamp the float from either side of the robotic fish to allow electrical connections on the sides. This float was attempted to manufacture but it failed due to the dimensional intricacies leading to the final float design that was adopted in developing the robotic fish.

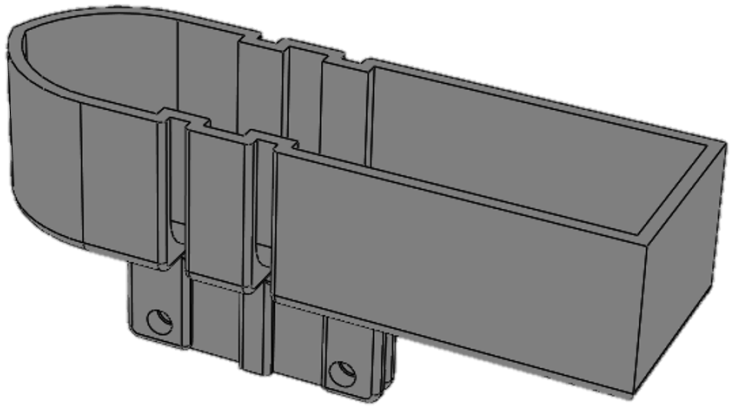

Figure A.2: Float adapted for final testing

Figure A.2 shows the final design which was designed to cater to two main functionalities. First, to balance buoyant forces and secondly to make pathways for electrical connections. This was manufactured by 3D printing technique using PLA material.

The dimensions of the float was decided based on the volume required to generate the required buoyant forces to counter the weight of the robotic fish. If $F_g$ is the gravitational force acting downwards and $F_b$ is the buoyant force, $F_b$ should be greater than or equal to $F_g$ to prevent the fish from sinking to the bottom of the tank.

$F_g = \rho_{rf} * V_{rf} * \mathrm{g}$

The average density, $\rho_{rf}$ of the robotic fish is considered to be $1.5 g/cm^3$ based on the average density of the materials used, while the fish occupies a volume $V_{rf}$ of $2400 mm^3$.

As, $F_b = \rho_w * V_w * \mathrm{g}$

where $\rho_w$ is the density of the water ( $1 gm/cm^3$) and $V_w$ is the volume of water displaced by the robotic fish. On calculating for the volume of water displaced by the , $V_w = 3600 mm^3$.

Thus, the volume of float should be more than $3600 mm^3$. However, considering a factor of 2.5, the float was designed with a volume of $9000 mm^3$ with dimensions $13mm \times 15mm \times 46mm$. The factor of 2.5 was considered as the float would be routed with electrical connections adding to the weight that had to be balanced.

# B

# Safety Assessment of Carbon Black Ink

The two types of carbon black inks that could be used for printing electrodes were JR-700 HV and JR-700 LV ink from Novacentrix. The ink comprised of carbon nano-particles and hence was assessed to abide by the safety to ensure the exposure during working hours remained within the limits as mentioned in the datasheet.

The code used to evaluate the concentration of nanoparticles in the lab while working for certain hours is described below. The datasheet of the inks can be found on the Novacentrix website which gives details of the particle size and exposure limtis.

```
%HV ink

sig1 = 59.11 ; %std deviation

mu1= 117.2 ; %avg size

x1 = 40 ; %initial size

x2 = 100 ; %final size

HV = 10 ; %gm of carbon in HV ink

% p = @(x) 1/(sig*sqrt(2*pi))*exp(-(x-mu).2/(2*sig2)) ; % probablity function

Q1 = integral(@(x) 1/(sig1*sqrt(2*pi))*exp(-(x-mu1).2/(2*(sig12))),x1,x2) ; %probablity of nanopar-
ticles

AmountHV = Q1*HV % amount of carbon nanoparticles in the ink

%LV ink

sig2 = 52.66 ; %std deviation

mu2= 120.6 ; %avg size

x3 = 40 ; %initial size

x4 = 100 ; %final size

LV = 10 ; %gm of carbon in LV ink

Q2 = integral(@(x) 1/(sig2*sqrt(2*pi))*exp(-(x-mu2).2/(2*(sig22))),x3,x4) ; %probablity of nanopar-
```

ticles

AmountLV = Q2*LV % amount of carbon nanoparticles in the ink

The amount of carbon nanoparticles calculated using this code should be within the exposure limits as suggested in the datasheet.

# C

# Electrode Patterns

The electrodes are produced as images in the PNG file format as depicted in the images below. Each image is of dimensions $70mm$ x $25mm$. In order to print the electrodes of the actuator, an index pattern is printed first on the substrate to match the position of other electrodes on the substrate. While manufacturing uni-morph actuators, only the left side electrodes were printed. The printed actuator samples were then laser cut into the desired shape using the same index pattern as seen in Figure C.1.

Figure C.1: Index pattern

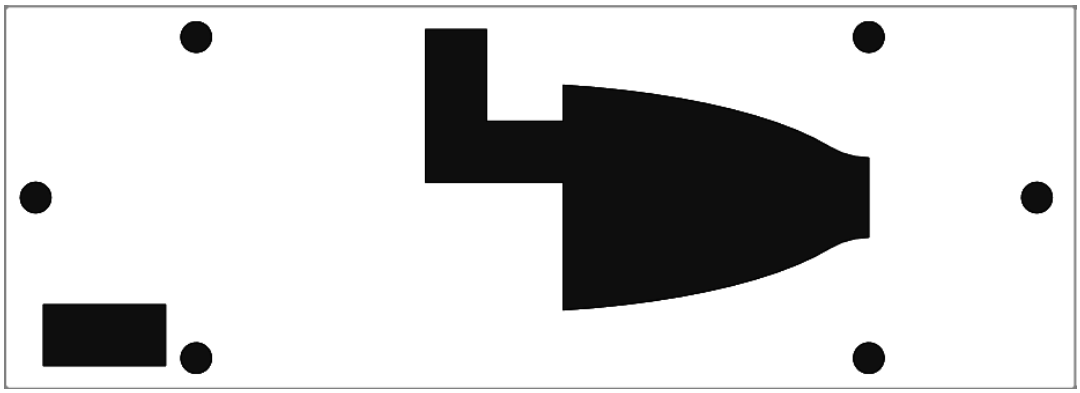

Figure C.2: Left side bottom electrode pattern

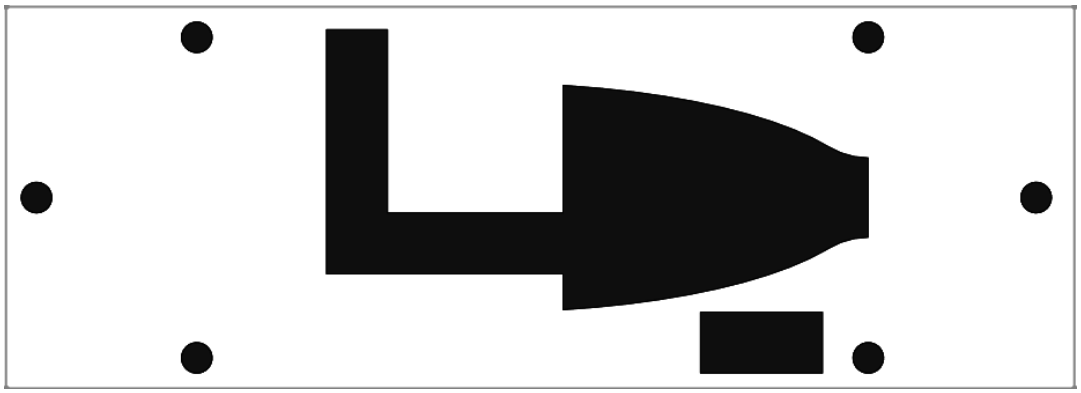

Figure C.3: Left side top electrode pattern

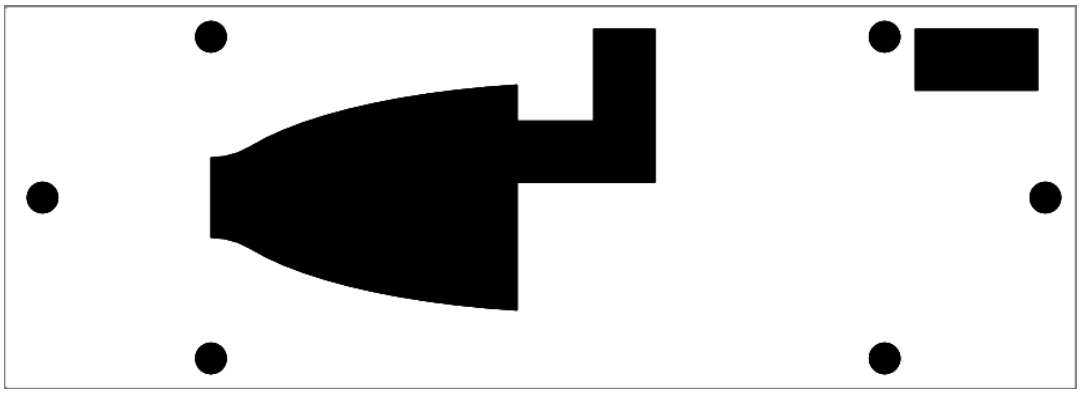

Figure C.4: Right side bottom electrode pattern

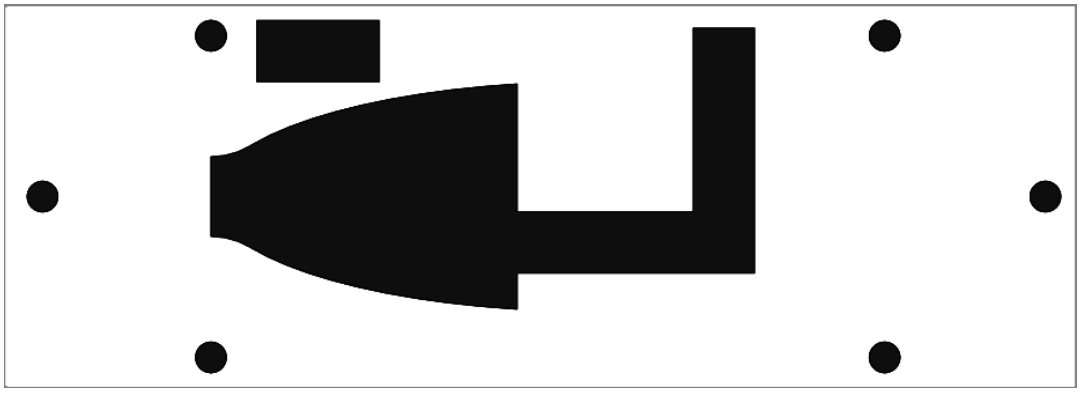

Figure C.5: Right side top electrode pattern

# D

# Performance Evaluation by Manual Tracking

This appendix presents the code that was developed to manually track the robotic fish from a video recorded while swimming to estimate the velocity. Although it was not used as the robotic fish sample prototypes were not successfully propelling, this code could be used in the future. The code allows the user to import a video in *.MP4 format and generates frames from the video. The manual tracking facility allows the user to track the desired point on the video frame which generates position coordinates. This could further be plotted to analyze the swimming pattern and velocity of the robot. The MATLAB code for evaluating the performance is given below:

```
clear all;

clc;

vid = VideoReader('one.mp4');

numFrames = vid.NumberOfFrames;

n=numFrames;

k=0;

q=0;

for i = 1:100:n

frames = read(vid,i); %reading particular frames from video

imwrite(frames,['Image' int2str(i), '.jpg']); % changing frames to .jpg image files

k = k+1;

im(k)= image(frames); %displaying frames that are considered

[x,y,button]= ginput(1); % getting manual input from images displayed

q = q+1;

x_n(q) = x(1); % save all points you continue getting
```

$y_n(q)$ = y(1);

end

plot($x_n$,$y_n$,'r') % plotting coordinates

# Bibliography


[1] Robot reef protector sees a new way to check great barrier reef health. https://phys.org/news/2018-08-robot-reef-protector-great-barrier.html, . Accessed: 2020-01-29.

[2] Eggs exhibiting at nor-shipping 2019. https://eggsdesign.com/stories/read/eggs-exhibiting-at-nor-shipping-2019, . Accessed: 2020-01-29.

[3] Consent form | scuba diving. https://www.scubadiving.com/drive-and-dive-exploring-wrecks-tobermory, . Accessed: 2020-01-29.

[4] Convenzione sorrento-terna per investimenti in opere di pubblica utilità - telestreet arcobaleno. https://telestreetarcobaleno.tv/convenzione-sorrento-terna-per-investimenti-in-opere-di-pubblica-utilita/, . Accessed: 2020-01-29.

[5] Keith Baelz. P(VDF-TrFe-CTFE) actuators with inkjet printed electrodes. 2019.

[6] Frédéric Boyer, Mathieu Porez, Ferhat Morsli, and Yannick Morel. Locomotion dynamics for bio-inspired robots with soft appendages: Application to flapping flight and passive swimming. *Journal of Nonlinear Science*, 27(4):1121–1154, 2017.

[7] Peter Buzzacott. *DAN Annual Diving Report 2017 Edition: A Report on 2015 Diving Fatalities, Injuries, and Incidents*. Divers Alert Network, 2017.

[8] Peter Buzzacott and Divers Alert Network. Dan annual diving report. *Divers Alert Network: Durham, NC, USA*, 2015.

[9] Di Chen, Weiping Shao, and Chunquan Xu. Development of a soft robotic fish with bcf propulsion using mfc smart materials. In *2018 37th Chinese Control Conference (CCC)*, pages 5358–5363. IEEE, 2018.

[10] Won-Shik Chu, Kyung-Tae Lee, Sung-Hyuk Song, Min-Woo Han, Jang-Yeob Lee, Hyung-Soo Kim, Min-Soo Kim, Yong-Jai Park, Kyu-Jin Cho, and Sung-Hoon Ahn. Review of biomimetic underwater robots using smart actuators. *International journal of precision engineering and manufacturing*, 13(7):1281–1292, 2012.

[11] Ahmad Athif Mohd Faudzi, Muhammad Rusydi Muhamamad Razif, Naja Aimi Mohd Nordin, Elango Natarajan, and Omar Yaakob. A review on development of robotic fish. *Journal of Transport System Engineering*, 1(1):12–22, 2014.

[12] Lindsey Hines, Kirstin Petersen, Guo Zhan Lum, and Metin Sitti. Soft actuators for small-scale robotics. *Advanced materials*, 29(13):1603483, 2017.

[13] Chan Hoang Le, Quang Sang Nguyen, and Hoon Cheol Park. A sma-based actuation system for a fish robot. *Smart Structures and Systems*, 10(6):501–515, 2012.

[14] Zakai J Olsen and Kwang J Kim. Design and modeling of a new biomimetic soft robotic jellyfish using ipmc-based electroactive polymers. *Frontiers in Robotics and AI*, 6:112, 2019.

[15] Aditi Raj and Atul Thakur. Fish-inspired robots: design, sensing, actuation, and autonomy—a review of research. *Bioinspiration & biomimetics*, 11(3):031001, 2016.

[16] Mohsen Shahinpoor and Kwang J Kim. Ionic polymer–metal composites: Iii. modeling and simulation as biomimetic sensors, actuators, transducers, and artificial muscles. *Smart materials and structures*, 13 (6):1362, 2004.

[17] WY Tey and NA Che Sidik. Comparison of swimming performance between two dimensional carangiform and anguilliform locomotor. *Journal of Advanced Research in Fluid Mechanics and Thermal Sciences*, 11:1–10.

[18] Wenjing Zhao, Aiguo Ming, and Makoto Shimojo. Development of high-performance soft robotic fish by numerical coupling analysis. *Applied Bionics and Biomechanics*, 2018, 2018.